

Differential Cofactor Requirements for Histone Eviction from Two Nucleosomes at the Yeast *PHO84* Promoter Are Determined by Intrinsic Nucleosome Stability[∇]

Christian J. Wippo,¹ Bojana Silic Krstulovic,² Franziska Ertel,¹ Sanja Musladin,² Dorothea Blaschke,¹ Sabrina Stürzl,¹ Guo-Cheng Yuan,³ Wolfram Höz,^{1†} Philipp Korber,^{1*} and Slobodan Barbaric²

*Adolf-Butenandt-Institut, Universität München, Munich, Germany*¹; *Laboratory of Biochemistry, Faculty of Food Technology and Biotechnology, University of Zagreb, Zagreb, Croatia*²; and *Department of Biostatistics, Harvard School of Public Health, and Department of Biostatistics and Computational Biology, Dana-Farber Cancer Institute, Boston, Massachusetts*³

Received 4 July 2008/Returned for modification 6 August 2008/Accepted 1 March 2009

We showed previously that the strong *PHO5* promoter is less dependent on chromatin cofactors than the weaker coregulated *PHO8* promoter. In this study we asked if chromatin remodeling at the even stronger *PHO84* promoter was correspondingly less cofactor dependent. The repressed *PHO84* promoter showed a short hypersensitive region that was flanked upstream and downstream by a positioned nucleosome and contained two transactivator Pho4 sites. Promoter induction generated an extensive hypersensitive and histone-depleted region, yielding two more Pho4 sites accessible. This remodeling was strictly Pho4 dependent, strongly dependent on the remodelers Snf2 and Ino80 and on the histone acetyltransferase Gcn5, and more weakly on the acetyltransferase Rtt109. Importantly, remodeling of each of the two positioned nucleosomes required Snf2 and Ino80 to different degrees. Only remodeling of the upstream nucleosome was strictly dependent on Snf2. Further, remodeling of the upstream nucleosome was more dependent on Ino80 than remodeling of the downstream nucleosome. Both nucleosomes differed in their intrinsic stabilities as predicted in silico and measured in vitro. The causal relationship between the different nucleosome stabilities and the different cofactor requirements was shown by introducing destabilizing mutations in vivo. Therefore, chromatin cofactor requirements were determined by intrinsic nucleosome stabilities rather than correlated to promoter strength.

Nuclear eukaryotic DNA is packaged into nucleosomes, where DNA is wrapped around a protein core consisting of eight histone proteins (48). The nucleosome forms the basic unit of a complex protein-nucleic acid structure termed chromatin. Chromatin structure has a strong influence on the regulation of gene transcription as the accessibility of DNA regions, for example, promoter elements and transactivator binding sites, is restricted and modulated by their incorporation into nucleosomes. Therefore, it has become an important field of research to understand the mechanisms by which transcription activators or repressors and the transcriptional machinery gain access to their binding sites and navigate the chromatin environment (51).

Many yeast nucleosomes are clearly positioned in relation to the DNA sequence (45, 49, 67, 82, 85), and nucleosomes are shown to occlude transactivator binding sites (47, 80). Nonetheless, it has become clear that nucleosomes, despite their intrinsic mostly repressive function, are highly dynamic. Especially in yeast promoter regions, there is a constant turnover of histones (20, 34, 62). The dynamics of chromatin are mediated by an intricate interplay of chromatin-related cofactors. For example, the so-called remodeling complexes, like the SWI/SNF, Ino80, or ISWI complexes, use the energy of ATP to either slide nucleosomes along the DNA, to alter the nucleo-

some structure to provide more accessible DNA, to exchange histones from the octamer core for variant histones, or even to completely disassemble nucleosomes and evict the histones from the previously nucleosomal region (10, 24, 46, 79). Remodeling complexes work in concert with a great variety of histone-modifying enzymes that add or remove chemical modifications like acetyl, methyl, or phosphate residues (11, 40). Further, free histones that are not part of a nucleosome are highly aggregation prone and are therefore bound by a diverse group of histone chaperones that assist nucleosome assembly and disassembly (56). At present it is not possible to predict which chromatin cofactors are required for chromatin remodeling in a particular case, as no comprehensive rules for cofactor requirements have been established.

The yeast *PHO5* promoter is a classical example for the role of chromatin in promoter regulation (74). Upon induction, an array of four positioned nucleosomes at the repressed promoter becomes mostly remodeled, leading to an extended nuclease-hypersensitive site that is largely depleted of histones (3, 14, 58). That way an additional binding site for the specific transactivator Pho4 becomes accessible, which is a critical prerequisite for gene induction (25, 26). The *PHO8* promoter is coregulated by the same transactivator as *PHO5* and also shows a pronounced chromatin transition upon induction (5) but has much lower promoter strength, i.e., the transcriptional activity in the fully induced state is much lower (52). In the past, we and others studied extensively the mechanisms that lead to promoter chromatin opening at these two promoters. At both promoters the SWI/SNF and Ino80 remodeling complexes, the histone acetyltransferase Gcn5, and the histone

* Corresponding author. Mailing address: Adolf-Butenandt-Institut, Universität München, Schillerstr. 44, 80336 Munich, Germany. Phone: 49-89-218075435. Fax: 49-89-218075425. E-mail: pkorber@lmu.de.

† Deceased, 13 November 2005.

∇ Published ahead of print on 23 March 2009.

chaperone Asf1 are involved in chromatin remodeling (6). However, the degree of cofactor requirement is markedly different. Whereas the *PHO8* promoter strictly depends on the ATPase subunit Snf2 of the SWI/SNF complex and on Gcn5 for promoter opening (28), there are redundant pathways for *PHO5* promoter chromatin remodeling, and no essential cofactor downstream of the transactivator Pho4 has been identified yet (6). Previously, we suggested that different intrinsic stabilities of promoter nucleosomes could be the reason for the differential cofactor requirement at these two promoters (31). Now, we wondered if it was a general trend that stronger promoters are packaged into less stable nucleosomes and show less dependency on chromatin cofactors.

In order to address this question without further complication by comparing different transactivation mechanisms, we turned to the *PHO84* promoter, which is coregulated with the *PHO5* and *PHO8* promoters but is even stronger than the *PHO5* promoter (54). The *PHO84* gene encodes a high-affinity phosphate transporter (15), and its mechanism of transcriptional regulation via regulation of Pho4 activity, as it is common to the phosphate-regulated genes, is mostly known (35, 37, 55). A comparative study of the transcriptional induction of the two coregulated *PHO5* and *PHO84* genes in response to phosphate starvation showed a lower threshold for *PHO84* induction. Cells grown in medium with intermediate phosphate concentrations activate transcription of *PHO84* but not of *PHO5* (71). Even growth in rich yeast extract-peptone-dextrose (YPD) medium, which is mostly repressive for *PHO5* induction, leads to significant levels of *PHO84* transcription (23, 53). Also, the induction of *PHO84* occurs more rapidly than induction of *PHO5*. However, this is not an intrinsic feature of the *PHO84* promoter but a consequence of the lower threshold of induction. Polyphosphate stores in the cell buffer the physiological signaling pathway of phosphate starvation, leading to a gradual increase in signal strength and an earlier response of the *PHO84* promoter than of the *PHO5* promoter. Mutants that are defective in polyphosphate storage induce *PHO5* and *PHO84* with similar kinetics (77).

The role of chromatin in the regulation of the *PHO84* promoter has not been explicitly studied yet. Nonetheless, there are several reports on effects of chromatin-related cofactors on the activity of *PHO84* under repressing or inducing conditions. This argues that also the *PHO84* promoter is regulated on the level of chromatin structure and makes it a promising model for the study of promoter chromatin remodeling mechanisms.

Genome-wide expression analyses in rich YPD medium revealed that *PHO84* is downregulated in the absence of Gcn5 or Snf2 (44). Shukla et al. (68, 69) demonstrated reduced acetylation of histone H3 and reduced recruitment of TATA binding protein and polymerase II at the *PHO84* promoter under such conditions in a *gcn5* mutant. The recruitment of Snf2 to the *PHO84* promoter in YPD medium has been directly shown, and this recruitment is dependent on Pho4 and vice versa (23). Also, both Snf2 and Ino80 are present at the induced *PHO84* promoter, and induced *PHO84* mRNA levels are reduced in the absence of these cofactors (36, 72). Further, basal transcription is increased in the absence of the histone methyltransferase Set1 (16). Very recently, during preparation of the manuscript, a comprehensive study of PHO regulon promoters explained very convincingly that the low threshold of *PHO84*

induction and its high dynamic range are due to the affinities of the five Pho4 binding sites and their positions in relation to positioned nucleosomes at the *PHO84* promoter (41). That study also showed that *PHO84* promoter nucleosomes become remodeled upon induction, but the role of chromatin cofactors was not addressed.

We have now characterized the chromatin states at the *PHO84* promoter under repressing and inducing conditions and present findings of our comprehensive investigation of the role of Pho4 binding sites, i.e., UASp elements, and chromatin cofactors in *PHO84* promoter chromatin dynamics. The *PHO84* promoter in the repressed state exhibited a short hypersensitive region that was flanked by two positioned nucleosomes and harbored two high-affinity Pho4 binding sites. Upon induction, this chromatin structure was remodeled into an extensive hypersensitive region that was depleted of histones and allowed access to two additional UASp elements. This chromatin transition was strongly dependent on Snf2, Ino80, and Gcn5, weakly dependent on the histone acetyltransferase Rtt109, and even more weakly on the histone chaperone Asf1. Strikingly, remodeling of each of the two nucleosomes flanking the short hypersensitive region in the repressed state showed a markedly different degree of cofactor requirement. Remodeling of one was critically dependent on Snf2, whereas remodeling of the other one was not. In addition, remodeling of the latter was less dependent on Ino80 than remodeling of the former and was even remodeled in the simultaneous absence of both Snf2 and Ino80. Therefore, the strong *PHO84* promoter appeared to be a hybrid between the *PHO5* and *PHO8* promoters with regard to the presence of both a stable, strictly Snf2 dependent nucleosome and a less stable, redundantly remodeled nucleosome at the same promoter. We show that this differential cofactor requirement was caused by different intrinsic stabilities of the two nucleosomes, as manipulation of nucleosome stability resulted in corresponding changes in the degree of remodeling cofactor requirements. We suggest that cofactor requirements for remodeling of promoter nucleosomes are mainly determined by intrinsic stabilities of individual nucleosomes and that promoter strength is not stringently predictive for cofactor requirements.

MATERIALS AND METHODS

Strains and media. For a complete list of the *Saccharomyces cerevisiae* strains used in this study see Table 1. Strain CY338 is a derivative of CY337 where the *PHO4* locus was disrupted by transformation with a linear DNA fragment of the *PHO4* locus with a *URA3* marker gene cassette inserted into the *PHO4* open reading frame (ORF). CY339, CY409, and other *pho5* derivatives of strains were constructed by transformation with a linear fragment that inserted a *URA3* cassette instead of the BamHI-SalI fragment at the *PHO5* locus. Yeast strains were grown under repressive conditions (high phosphate [+P_i]) in YPD with 0.1 g/liter adenine plus 1 g/liter KH₂PO₄, in yeast nitrogen base selection medium supplemented with the required amino acids for plasmid-bearing strains, and in phosphate-free synthetic medium for induction (3, 6).

Plasmids. The plasmids pCB84a and pCB84b are derivatives of pCB/WT (26) in which a *LEU2* marker cassette is inserted into the HindIII site and where the *PHO5* promoter is exchanged for the *PHO84* promoter. In more detail, a PCR product, generated with the primers PHO84(do) (5'-AGATTTAAACATTGGATTGTATTCGTGG-3') and either PHO84(up-885) (5'-CAGGATCCAAAGTGTACACGTG-3') for pCB84a or PHO84(up-479) (5'-CAGGATCCCGTTCCTCTCACTG-3') for pCB84b and genomic DNA as template, was ligated via BamHI and DraI into the *PHO5* promoter. As there are multiple DraI sites in the vector, the vector was opened via BamHI and SalI and the DraI-SalI fragment 5' of the *PHO5* ORF was prepared separately and added to the ligation mixture, resulting in a triple ligation

TABLE 1. *Saccharomyces cerevisiae* strains used in this study

Strain	Genotype	Source	Reference		
CY337	<i>MATa ura3-52 lys2-801 ade2-101 leu2-Δ1 his3-Δ200</i>	P. Hieter and C. L. Peterson	60		
CY338	CY337 <i>pho4::URA3</i>	Our group			
CY339	CY337 <i>pho5::URA3</i>				
CY396	<i>MATα swi2Δ::HIS3 SWI2-HA-6HIS::URA3 HO-lacZ</i>	C. L. Peterson	60		
CY397	<i>MATα swi2Δ::HIS3 swi2(K798A)-HA-6HIS::URA3 HO-lacZ</i>	Our group	6		
CY407	CY337 <i>snf2::HIS3</i>				
CY407 <i>ino80</i>	CY407 <i>ino80::URA3</i>				
CY409	CY407 <i>pho5::URA3</i>				
CY53379 <i>pho5</i>	CY337 <i>gcn5::ura3</i> (URA3 function lost on 5-fluoroorotic acid) <i>pho5::URA3</i>			28	
BY4741-0	wt	X. Shen	66		
BY4741-1	BY4741-0 <i>ino80::HIS3</i>				
Y00000 (same as BY4741)	<i>MATa his3Δ1 leu2Δ0 met15Δ0 ura3Δ0</i>	EUROSCARF	http://web.uni-frankfurt.de/fb15/mikro/euroscarf/		
Y01490	BY4741 <i>rtt109::kanMX4</i>				
Y01310	BY4741 <i>asf1::kanMX4</i>	A. Verreault			
W303a	<i>MATa leu2-3,112 ura3-1 his3-11,15 trp1-1 ade2-1 can1-100</i>				
W303a <i>asf1</i> (same as MAR 101)	W303a <i>asf1::kanMX</i>				
PKY4170	W303a <i>rtt109::kanMX bar1-1</i>			P. D. Kaufman	
PKY4182	W303a <i>rtt109::kanMX asf1::TRP1 URA3-VIIL</i>				
PKY4226	W303a <i>bar1-1 vps75::HIS3</i>	This study			
W303a <i>asf1 pho5</i>	W303a <i>asf1 pho5::URA3</i>				
PKY4170 <i>pho5</i>	PKY4170 <i>pho5::URA3</i>				
PKY4226 <i>pho5</i>	PKY4226 <i>pho5::URA3</i>				
FY1352	<i>MATa leu2Δ1 his3Δ200 ura3-52 lys2-173R2 snf2Δ::LEU2 gcn5Δ::HIS3</i>			F. Winston	61

of PCR product, BamHI-SalI-digested vector backbone, and the DraI-SalI fragment. Plasmid pCB84a was used as template for generating the UASp variants UASpCmut, -Dmut, and -Emut by the Megaprimer method (63) with the following primers that introduced the point mutations: PHO84-mutC, 5'-GCCAATTTAAT AGTTTCATCGATGATCAGTTATTTCCAGCAGCTG-3'; PHO84-mutD, 5'-GG ACGTGTTATTTCCACATCGATGGCGGAAATAGCGAC-3'; PHO84-mutE, 5'-GCTTATTAGCTAGATTAATACTAGTCTGTTACTCATTAAATTA AC-3'. The following primers were used as reverse primers for generating UASpCmut, -Dmut, and -Emut, respectively: PHO84-rev1, 5'-CCACAATAGTAA GTGG-3'; PHO84-rev2, 5'-CTGGTGATCTACGAG-3'. The point mutations introduced a ClaI site each instead of UASpC and UASpD and a SpeI site instead of UASpE. The combined mutations of UASpCmut and UASpDmut were generated by inserting the BsgI-MstII fragment from the UASpEmut plasmid into the UASpCmut and UASpDmut plasmids, respectively. The UASpBmut plasmid and plasmid pCB84a-10A were generated using pCB84a as template and the QuikChange kit (Stratagene) with the following mutagenesis primers: pho84-mutBfor, 5'-GAAATGACAGCAATCAGTATTACGGAATTCGGTGTGTTATA GGCGCCCTATAC-3', and pho84-mutBrev, 5'-GTATAGGGCGCCTATA ACAGCACCAAAATCCGTAATACTAGTGTGCTATTTTC-3' for pCB84a-Bmut and pho84-A10for, 5'-GTATAGGGCGCCTATAACAGCACCAACGTGC GTAAAAAAAAGCTGTCATTTCTTGGCATGTTTTCT-3', and pho84-A10rev, 5'-AGAAAACATGCCAAGAAATGACAGCTTTTTTTTTTACGCAC GTTGGTGTGTTATAGGGCCCTATAC-3', for pCB84a-10A, respectively. The point mutation in pCB84a-Bmut introduced an EcoRI site instead of UASpB. Plasmid pCB84a-19A was generated with the QuikChange kit and pCB84a-10A as template and the primers pho84-A19for, 5'-TGCTGCACGTATAGGGCGCCTA TAACAGCACCAAAATAAAAAAAAAAAAAAAAAAGCTGTCATTTCTTGGCAT GTTTTC-3', and pho84-A19rev, 5'-GAAAACATGCCAAGAAATGACAGCTT TTTTTTTTTTTTTTGGTGTGTTATAGGGCGCCTATACGTGACGCA-3'. Plasmid pUC19-PHO84 was prepared by ligating a 3.5-kb PCR product, generated with the primers 5'-CCGGAATTCGAGTCATGATTTGGAAACAGCTC C-3' and 5'-CGCGGATCCGAGAGATGTGAGGAAAT-3' and genomic DNA from strain BY4741 as template, via EcoRI and BamHI, into pUC19. Plasmids pUC19-PHO84-10A and -19A were generated from pUC19-PHO84 and from pUC19-PHO84-10A with the primers pho84-A10for/rev and pho84-A19for/rev, respectively, and the QuikChange kit. The DNA sequence of the *PHO84* promoter region in all plasmids constructed in this study was confirmed by dideoxy sequencing (data not shown). The Pho4 overexpression plasmid pP4-70L corresponds to YeP4 (75) but carries the *LEU2* instead of the *URA3* marker.

Functional assays and chromatin analysis. Acid phosphatase assays were done as described previously (29). The preparation of yeast nuclei (3) and chromatin analysis of nuclei by restriction nucleases and DNase I digestion with indirect end labeling were as described previously (27, 76). Secondary cleavage for DNase I indirect end labeling was done with HindIII for both the chromosomal and the plasmid locus (at bp -1453 and -1239 from the ATG of the *PHO84* ORF for chromosomal and plasmid locus, respectively). For secondary cleavage after chromatin digestion with BsrBI, HhaI, MfeI, PacI, AgeI, SpeI, and FokI, we used HindIII for the chromosomal locus and HindIII/SalI for the plasmid locus. The probe for the chromosomal locus is a PCR product corresponding to bases -1428 to -1083 from the ATG of the *PHO84* ORF, and the probe for the plasmid locus corresponds to the HindIII-BamHI fragment of pBR322. Due to the presence of multiple HhaI sites in the plasmid probe region, i.e., the HindIII-BamHI fragment of pBR322, BamHI and EcoRV were used for secondary cleavage and a PCR product from -557 to -310 was used as probe in order to monitor HhaI accessibility at the plasmid locus. Due to the frequent occurrence of TaqI sites, AvaII/ClaI were used for the chromosomal and BamHI/SalI for the plasmid locus for secondary cleavage and a PCR product from -736 to -371 was used as a probe for monitoring TaqI accessibilities.

ChIP analysis. Yeast cultures with a density of 1×10^7 to 2×10^7 cells/ml were treated with 1% formaldehyde for 20 min at room temperature. Cross-linking was quenched by adding glycine to a final concentration of 125 mM. The cells were washed two times with ice-cold 0.9% NaCl, resuspended in HEG150 buffer (150 mM NaCl, 50 mM HEPES, pH 7.6, 10% glycerol, 1% Triton X-100, 1 mM EDTA, 1 mM dithiothreitol [DTT], 1 mM phenylmethylsulfonyl fluoride) and lysed with a French press (three times at 1,100 lb/in²) or by sonication (Bioruptor; Diagenode; three times for 30 s with a 60-s pause, position high, ice water bath). In this last step, chromatin was sheared to an average size of 500-bp fragments. Chromatin immunoprecipitation (ChIP) was performed as described before (73). The anti-histone H3 C-terminal antibody was obtained from Abcam (ab1791-100). Immunoprecipitated DNA was quantitatively measured in triplicates with the ABI Prism 7000 sequence detection system using the following amplicons: TEL-1, 5'-TCCGAACGCTATTCCA GAAAGT-3'; TEL-B, 5'-CCATAATGCCTCTATATTTAGCCTTT-3'; TEL-probe, 5'-6-carboxyfluorescein [FAM]-TCCAGCCGCTTGTAACTCTCCGACA-6-carboxytetramethylrhodamine (TAM)-3'; ACT1-A, 5'-TGGATTCCGGTGATGGT GTT-3'; ACT1-B, 5'-TCAAAATGGCGTGAGGTAGAGA-3'; ACT1-probe, 5'-FAM-CTCACGTCGTTCCAATTTACGCTGGTTT-TAM-3'; PHO84 UASpC-A, 5'-GAAAAACACCCGTTCTCTACT-3'; PHO84 UASpC-B, 5'-CCCAGTG

CTGGAAATAACAC-3'; *PHO84* probe, 5'-FAM-CCCAGTCCCAATTTAATAGT TCCACGTG-TAM-3'.

Salt gradient dialysis chromatin assembly. Salt gradient dialysis was performed as described previously (42). A typical assembly reaction mixture contained 10 μ g supercoiled plasmid DNA (Qiagen preparation), 20 μ g bovine serum albumin (A-8022; Sigma), and variable amounts (for example, 6 or 10 μ g) of *Drosophila melanogaster* embryo histone octamers (70) in 100 μ l high-salt buffer (10 mM Tris-HCl, pH 7.6, 2 M NaCl, 1 mM EDTA, 1 mM β -mercaptoethanol, 0.05% Igepal CA630 [I-3063; Sigma]) and was dialyzed for 15 h at room temperature while slowly diluting 300 ml of high-salt buffer with 3 liters of low-salt buffer (same as the high-salt buffer, but with 50 mM NaCl) using a peristaltic pump. A final dialysis step versus low-salt buffer ensured a final NaCl concentration of 50 mM.

Yeast whole-cell extract preparation. Yeast whole-cell extract was prepared as previously described (31) with the following modifications. Commercially available baker's yeast concentrate (Deutsche Hefewerke GmbH, Nürnberg, Germany) was used as starting material for an upscaled version of the preparation. The extraction buffer was modified to 0.2 M HEPES-KOH, pH 7.5, 10 mM MgSO₄, 10% glycerol, 1 mM EDTA, 390 mM (NH₄)₂SO₄, 1 mM DTT, and 1 \times Complete protease inhibitor without EDTA (Roche Applied Science), and the buffer for resuspension after the ammonium sulfate precipitation was 20 mM HEPES-KOH, pH 7.5, 10% glycerol, 80 mM KCl, 1 mM EGTA, 5 mM DTT, and 1 \times Complete protease inhibitor without EDTA. For the final dialysis the same buffer as for resuspension but with 0.1 mM phenylmethylsulfonyl fluoride and 1 mM sodium metabisulfite instead of the Complete protease inhibitor was used and exchanged to completion.

In vitro chromatin reconstitution. A 100- μ l reconstitution reaction mixture with 1 μ g DNA preassembled by salt gradient dialysis was incubated with or without yeast extract (~250 μ g protein, judged from Coomassie-stained gel lanes in comparison to standard protein) and with or without a regenerative energy system (3 mM ATP-MgCl₂, 30 mM creatine phosphate [Sigma], and 50 ng/ μ l creatine kinase [Roche Applied Science]) in assembly buffer (20 mM HEPES-KOH, pH 7.5, 10% glycerol, 80 mM KCl, 0.5 mM EGTA, 2.5 mM DTT) for 2 h at 30°C.

DNase I indirect end labeling and restriction enzyme accessibility assay for in vitro-reconstituted chromatin. Aliquots (25 μ l) of a reconstitution reaction mixture were mixed with an equal volume of digestion buffer (20 mM HEPES-KOH, pH 7.5, 12% glycerol, 5.5 mM MgCl₂, 5.5 mM CaCl₂, 2.5 mM DTT, 80 mM NaCl, 0.1 mg/ml bovine serum albumin) containing DNase I (04716728001; Roche Applied Science) at a concentration in the range of 0.005 to 0.02 U/ml (free DNA), 0.02 to 0.1 U/ml (salt gradient dialysis chromatin), or 2 to 10 U/ml (salt gradient dialysis chromatin with extract) and incubated at room temperature for 5 min. The digestion reactions were stopped by adding 10 μ l of Stop buffer (10 mM EDTA, 4% sodium dodecyl sulfate), deproteinized by proteinase K digestion overnight, and ethanol precipitated. SspI (bp -1440 from the ATG of the *PHO84* ORF) was used for secondary cleavage instead of HindIII. For direct comparison between in vitro-reconstituted chromatin and in vivo chromatin (see Fig. 7A, below), SspI was used for all loci.

Prior to restriction enzyme digestions, ATP was removed from the reconstitution reaction mixtures to inhibit ATP-dependent remodeling during the restriction digestion by adding 0.1 U of apyrase (M0393L; New England Biolabs) to the reaction mixtures and incubating for 30 min at 37°C. Two-microliter aliquots of an apyrase-treated reconstitution reaction mixture were combined with 30 μ l of RE digestion buffer (20 mM HEPES-KOH, pH 7.5, 4.5 mM MgCl₂, 2.5 mM DTT, 80 mM NaCl, 0.5 mM EGTA) and treated with two different enzyme concentrations for each restriction enzyme, similar to the in vivo RE digests. The reactions were stopped by adding 7.5 μ l Stop buffer, deproteinized by proteinase K digestion overnight, and ethanol precipitated. Secondary cleavage was performed as described above for the chromosome locus.

RESULTS

The chromatin structure at the *PHO84* promoter undergoes extensive remodeling upon induction. We characterized the *PHO84* promoter chromatin structure under repressing conditions, i.e., in rich or synthetic medium with additional phosphate to ensure full repression, and under inducing conditions, i.e., synthetic phosphate-free medium. By DNase I indirect end-labeling analysis of the repressed state (+P_i) we detected a short hypersensitive (sHS) region (about 150 bp), roughly

between the MfeI and ApaI restriction sites, that was flanked by one positioned nucleosome upstream and one downstream (Fig. 1A and B, upstream nucleosome and downstream nucleosome). This sHS region contained two closely positioned high-affinity Pho4 binding sites, UASpC and UASpD, whereas the two low-affinity sites, UASpB and UASpE, were occluded by the positioned upstream and downstream nucleosomes, respectively (Fig. 1B) (54). In addition, we observed a broad hypersensitive region upstream of the BsrBI restriction site. Upon induction (-P_i), the upstream nucleosome and at least one nucleosome downstream of the sHS region were remodeled, leading to an extended hypersensitive (eHS) region of about 500 bp. Its upstream border was almost fused to the broad hypersensitive region and the downstream border faded into the core promoter region around the TATA box and the transcriptional start site (Fig. 1A and B; see also Fig. 4B, 5A, and 8A, below). This way UASpB and UASpE became accessible (Fig. 1B). Sometimes the eHS region appeared to contain a short region of lower DNase I accessibility between the MfeI and ApaI sites (see Fig. 4B and 8A), which may reflect Pho4 and recruited factors bound to UASpC and UASpD. In Fig. 1A the intensity of the broad hypersensitive region upstream of the BsrBI site appeared to change somewhat upon induction, which was probably attributable to an overall lower degree of digestion. However, in the majority of cases it did not undergo major changes upon induction (see Fig. 4B, 5A, and 8A, -P_i panels, below; also, data not shown). Therefore we refer to it as a constitutive hypersensitive region (cHS).

The chromatin transition was fully dependent on the transactivator Pho4, as the *PHO84* promoter chromatin pattern under inducing conditions in a *pho4* deletion strain was virtually the same as the wild-type (wt) pattern of the repressed state (Fig. 1A). Interestingly, the unchanged nucleosome organization in a *pho4* mutant suggested that the nucleosome positioning at the repressed promoter did not depend on binding of Pho4, e.g., to its linker binding sites UASpC and UASpD.

In addition to DNase I indirect end labeling, we mapped the *PHO84* promoter chromatin structure of the repressed and the induced state more quantitatively by assaying the accessibility for several restriction enzymes along the promoter region that underwent the chromatin structure transition (Fig. 1C and D). Under +P_i conditions, the accessibilities for the various restriction enzymes were rather different, as would be expected for an organization into nucleosomes and nucleosome-free linker regions. The accessibilities at the HhaI and TaqI sites were the lowest, speaking for their protection by the upstream and downstream nucleosome, respectively. The BsrBI site was fully accessible under both repressing and inducing conditions, which was in agreement with its localization at the downstream start of the cHS region (Fig. 1A). The MfeI site was substantially but not fully accessible in the repressed state, indicating a location at the very border between the downstream nucleosome and the sHS region (Fig. 1A). Interestingly, a region of about 100 bp between the downstream nucleosome and the TATA box was only semiprotected in the repressed state, as the accessibilities for PacI, AgeI, and FokI were in the range of 43% (FokI) to 57% (AgeI) (Fig. 1C and D). This argued against a clearly positioned but rather for a less-organized nucleosome or for a chromatin structure with increased plas-

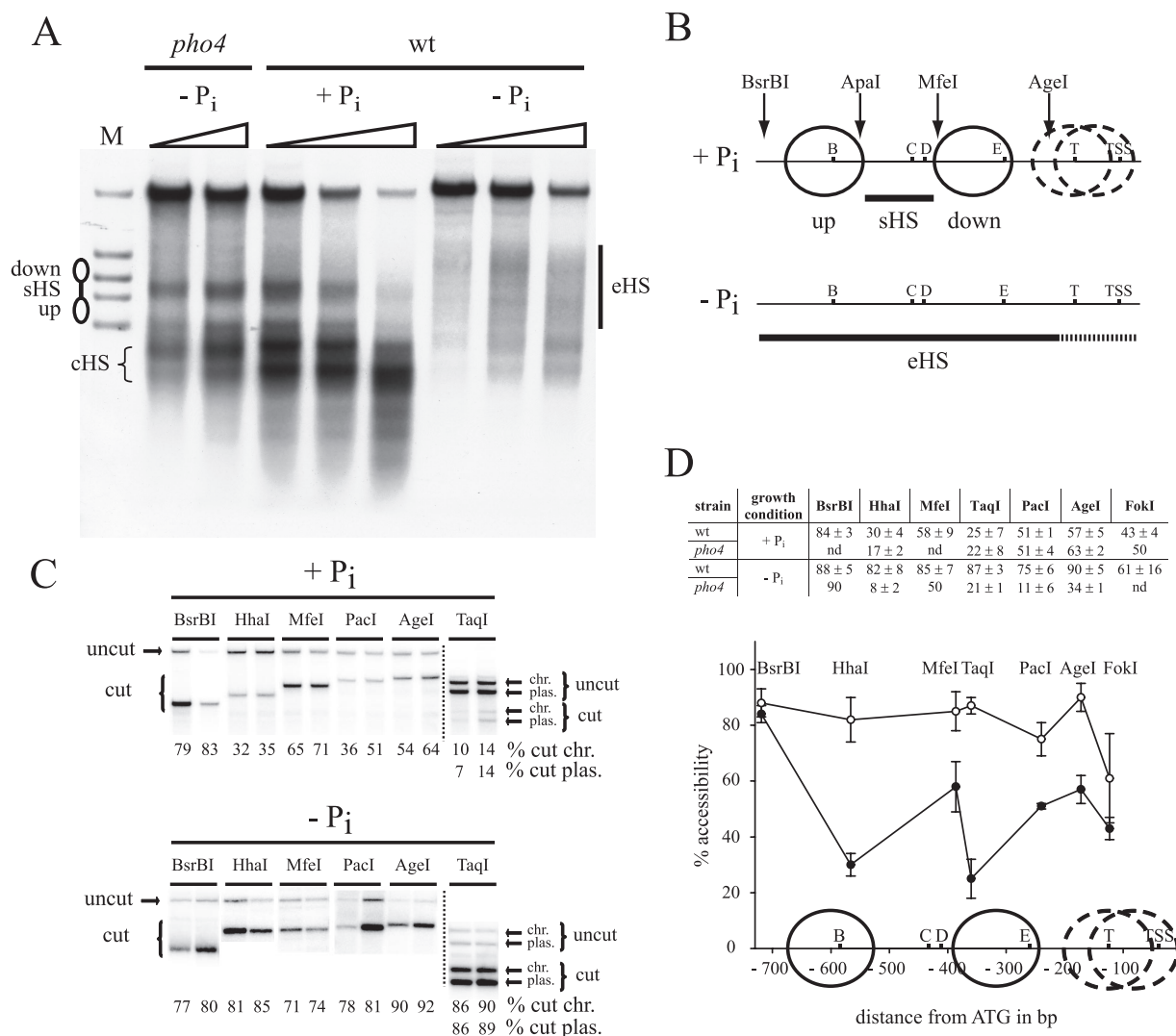


FIG. 1. The chromatin structure at the *PHO4* promoter undergoes extensive remodeling upon induction. (A) DNase I indirect end-labeling analysis of the chromatin structure at the chromosomal *PHO4* locus in wt (CY339 pCB84a) and *pho4* (CY338) strains grown in phosphate-containing medium (+P_i) or after overnight incubation in phosphate-free medium (-P_i). Ramps on top of the lanes designate increasing DNase I concentrations. The four marker fragments in the promoter region (lane M) were generated by double digests with HindIII and either AgeI, MfeI, ApaI, or BsrBI (from top to bottom in the lanes). The schematics on the left and right are analogous to the schematics of the +P_i and -P_i states in panel B, respectively. Down and up refer to positioned nucleosomes downstream and upstream of the sHS region, respectively. eHS denotes the extended hypersensitive region of the induced state, and cHS denotes the constitutive hypersensitive region. All samples were electrophoresed in the same gel, but for the -P_i data a stronger exposure is shown. (B) Schematic of the nucleosomal organization of the *PHO4* promoter in the repressed (+P_i) and induced (-P_i) state. Large circles denote the positioned nucleosomes (up and down) flanking the sHS (short horizontal bar). Stippled circles stand for a less-organized nucleosome structure with ambiguous positioning. The positions of four Pho4 binding sites (B to E, taken from reference 54), the TATA box (T, taken from reference 9), the transcriptional start site (TSS, taken from reference 50), and the four restriction sites used for generating marker fragments (see panel A) are indicated. Upon induction (-P_i), there is an eHS region (long horizontal bar) ranging from near the BsrBI up to the AgeI site and fading into the core promoter region (stippled horizontal bar). (C) Nuclei isolated from wt (CY339 pCB84a) cells grown under repressive (+P_i) or inducing (-P_i) conditions were digested with two different concentrations each of the indicated restriction enzymes and analyzed by indirect end labeling with probing for the chromosomal locus. Due to the specific probe and secondary cleavage for the analysis of TaqI accessibility, both the chromosomal (chr.) and the plasmid (plas.) locus were seen at the same time. Quantification of the percentage of cleaved DNA (% cut) was done by PhosphorImager analysis. The samples of the +P_i panel were electrophoresed on the same gel, but the samples of the -P_i panel were on different gels; therefore, the relative migration positions cannot be compared directly. (D) Average accessibility values of two to seven biological replicates and their standard deviations are given for the indicated restriction endonucleases and for wt (CY background) and *pho4* (CY338) strains under repressive (+P_i) or inducing (-P_i) conditions. nd, not determined. The wt data of the table (+P_i, closed circles; -P_i, open circles) are plotted versus the positions of the restriction sites relative to the ATG start codon. As for panel B, the positions of four Pho4 binding sites (B to E), the TATA box (T), and the transcriptional start site (TSS) are indicated on the x axis of the plot as well as the inferred positions of clearly positioned (large circles) and less-organized (overlapping stippled circles) nucleosomes.

ticity. Alternatively, some other DNA-protecting entity, e.g., an assembly of general transcription factors, could be responsible for this semiprotection.

In the induced state, all restriction enzyme sites tested in the promoter region of more than 500 bp upstream of the TATA box were highly accessible (Fig. 1C and D), confirming the presence of an extended hypersensitive region as observed by DNase I indirect end labeling (Fig. 1A) and suggesting that the whole region was mostly nucleosome free. Restriction enzyme accessibility assays also confirmed that the transition to this open chromatin state was dependent on Pho4 (Fig. 1D). For unknown reasons, the accessibilities at the HhaI, PacI, and AgeI sites, but not at the TaqI site, were even decreased under inducing compared to noninducing conditions in the *pho4* strain.

In the wt strain, the accessibility of the FokI cleavage site, which overlaps with the TATA box sequence (15), also increased upon induction, but not to the same high level as for the other restriction enzyme sites. In addition, the accessibility of the FokI site in the induced state was quite variable. This altogether may be due to the poor performance of this restriction enzyme on chromatin templates or may indicate the presence of an unstable or partially remodeled nucleosome or of components of the general transcription machinery recruited to the TATA box under inducing conditions.

In summary, the restriction enzyme accessibility data in connection with the DNase I indirect end-labeling analysis led us to map the upstream and downstream nucleosome as shown in Fig. 1B and D. The main guidelines were the location of the ApaI and MfeI sites just at the borders of the nucleosomes toward the sHS region. For the reasons stated above, we have not assigned clear nucleosomal positions to the region between the downstream nucleosome and the TATA box region but suggest a less-organized DNA protective structure there.

This less-organized structure together with the somewhat elevated accessibilities at the HhaI and TaqI sites suggested to us that there may be a low level of Pho4 present at the promoter even under repressive conditions. Under +P_i conditions Pho4 is mostly phosphorylated at multiple sites and mainly located in the cytosol (37), but some Pho4 may still be nuclear. For example, earlier we showed a Pho4 footprint at the repressed *PHO8* promoter (52) and *sin* mutations in histone H4 showed significantly derepressed *PHO5* activity in a UASp element-dependent, i.e., presumably Pho4-dependent, manner under otherwise-repressing conditions (81). Such nuclear Pho4 may bind especially to the accessible high-affinity sites UASpC and UASpD in the sHS region. This could lead to some basal recruitment of chromatin remodeling activities and a partially remodeled chromatin structure. We tested this by restriction enzyme analysis of the *PHO84* promoter region in a *pho4* deletion strain under high-phosphate conditions (Fig. 1D). However, only the accessibility of the HhaI site was decreased significantly, arguing that there was some basal Pho4-dependent remodeling only of the upstream nucleosome in the repressed state. This may also be noticeable based on the slightly more spread out sHS region in the presence of Pho4 (Fig. 1A, compare wt +P_i and *pho4* -P_i). In contrast, the structure between the downstream nucleosome and the TATA box region was maintained semiopen also in the absence of Pho4.

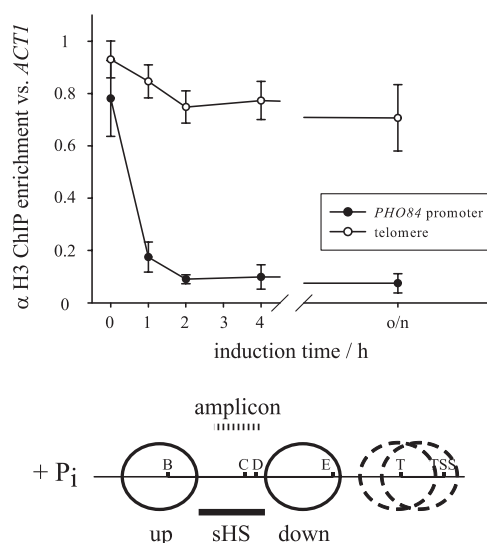


FIG. 2. Histones are depleted from the *PHO84* promoter region upon induction. The induction kinetics after transfer of a wt strain (CY337) to phosphate-free medium was followed by ChIP using a histone H3 C-terminal antibody and amplicons at the *PHO84* promoter, the telomere, and the *ACT1* open reading frame. ChIP data were normalized to input DNA and to the *ACT1* amplicon. Error bars show the standard deviations of three biological replicates. o/n, overnight induction. The scheme below the graph is analogous to Fig. 1B and shows the position of the *PHO84* promoter amplicon as a stippled bar.

Remodeling of *PHO84* promoter chromatin upon induction results in histone depletion from the promoter. The generation of an extended hypersensitive region at the induced *PHO84* promoter was reminiscent of our previous findings for the *PHO5* and *PHO8* promoters (3, 5). Such hypersensitivity was found by ourselves and others to reflect not just altered nucleosomal structures but also nucleosome disassembly leading to histone eviction from the promoter regions (1, 14, 38, 58). We checked if histones were lost also from the induced *PHO84* promoter. During *PHO84* induction kinetics, the histone H3 occupancy was monitored by ChIP using an antibody directed against the C terminus of histone H3. The histone H3 occupancy dropped after 2 hours of induction to about 10% of the level under repressing conditions (Fig. 2). At the same time there was no significant change of the histone H3 occupancy at a telomere control locus. Therefore, chromatin remodeling at the *PHO84* promoter eventually led to histone eviction.

The extent of chromatin remodeling critically depends on the intranucleosomal UASpE site. A special feature of the *PHO84* promoter is the presence of five Pho4 binding sites, UASpA to UASpE, which makes it one of the strongest PHO promoters (54). Ogawa et al. (54) showed previously by using a *P_{PHO84}-lacZ* reporter construct and deleting an extensive upstream region that UASpA and UASpB were not required for full *PHO84* activity. They further showed by site-directed mutagenesis that the low-affinity site UASpE in combination with either of the high-affinity sites UASpC or UASpD was necessary and sufficient for *PHO84* regulation. We wished to check if any of these effects on promoter activity actually reflected effects on chromatin remodeling.

We set up an analogous reporter system by constructing plas-

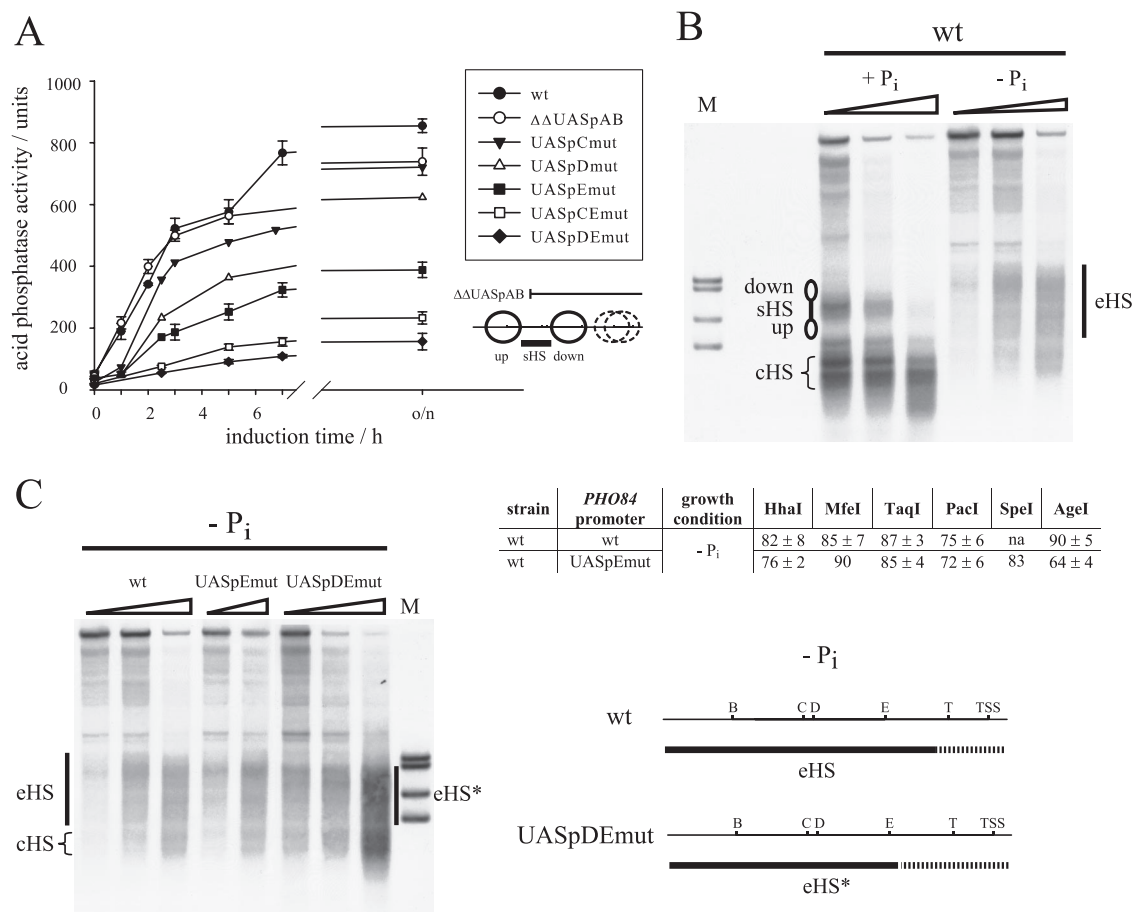


FIG. 3. Effects of Pho4 binding site deletions on *PHO84* promoter induction kinetics and chromatin remodeling. (A) The *PHO84* promoter induction kinetics after shift to phosphate-free medium was monitored in a *pho5* strain (CY339) bearing reporter plasmids where either the wt *PHO84* promoter (plasmid pCB84a), a truncated *PHO84* promoter leading to the deletion of UASpA and UASpB ($\Delta\Delta$ UASpAB; plasmid pCB84b), or promoter variants with point mutations in Pho4 binding sites (plasmids pCB84a-UASpCmut, -Dmut, -Emut, -CEmut, and -DEmut) were coupled to the *PHO5*-coding region. Thereby, the induction kinetics could be monitored by an acid phosphatase activity assay. Error bars show the standard deviations of at least three biological replicates. o/n, overnight induction. The scheme below the legend corresponds to the scheme in Fig. 1B, and the blunt end of the line above shows the point of truncation in the $\Delta\Delta$ UASpAB variant (plasmid pCB84b). (B) The chromatin transition between the repressed (+P_i) and induced (-P_i) states of the *PHO84* promoter on the pCB84a plasmid locus as monitored by DNase I indirect end labeling. The same blot as in Fig. 1A was stripped and rehybridized with the probe for the plasmid locus. Labeling is as for Fig. 1A, but the marker fragments (lane M) correspond to double digests with HindIII and either AgeI, SpeI, ApaI, or BsrBI (from top to bottom in the lane). The SpeI site was introduced upon mutating UASpE and therefore corresponds to the position of this site. (C) DNase I indirect end labeling and markers as for panel B for the plasmids pCB84a (wt), pCB84a-UASpEmut, and -DEmut, respectively, in strain CY339 under inducing conditions (-P_i). All samples were electrophoresed in the same gel, but for the UASpDE data a stronger exposure is shown. The table shows average accessibility values of the indicated restriction enzymes as in Fig. 1D. The wt data are the same as in Fig. 1D, and data for the UASpEmut promoter variant are derived from two biological replicates if a variation is given, na, not applicable. The schematics are analogous to Fig. 1B. eHS*, the less-extended hypersensitive region of *PHO84* promoter variants with mutated UASpE.

mid pCB84a, for which the *PHO84* promoter was coupled to the *PHO5* coding gene. Thereby we avoided possible chromatin structure artifacts due to the close presence of the bacterial *lacZ* DNA sequence (unpublished observations). The enzymatic activity of the secreted acid phosphatase Pho5 can be measured easily with intact cells and *PHO5* transcriptional activity fully correlates with acid phosphatase activity, indicating no significant posttranscriptional regulation of *PHO5* expression (8). Importantly, the endogenous copy of *PHO5* was always deleted in strains where *PHO84* reporter constructs were used.

Using the pCB84a construct we observed phosphate-regulated *PHO84* promoter activity with a substantially higher basal and final level of Pho5 acid phosphatase activity than seen with

the *PHO5* promoter (Fig. 3A; see also Fig. 9A and B, below). This was expected for the stronger *PHO84* promoter.

The *PHO84* promoter chromatin structure on the plasmid underwent the same regulated transition as the endogenous chromosomal locus (compare Fig. 3B and 1A for DNase I mapping; data not shown for restriction enzyme accessibilities). It should be noted that the region far upstream of the *PHO84* promoter, which is used for probing in indirect end-labeling techniques, was different between the plasmid and the chromosomal locus, thus allowing for a distinction of both loci within the same cell by differential probing and therefore excellent internal control. Due to the different relative position of the secondary cleavage site at the plasmid and chromosomal

locus, the DNase I indirect end-labeling fragments at the plasmid locus were 214 bp smaller, leading to a more stretched out appearance of the plasmid chromatin patterns on the blot. Possible minor changes in nucleosome positions between the chromosomal and the plasmid locus could still be undetected by this low-resolution approach.

Using this reporter plasmid, a set of promoter variants similar to the ones of Ogawa et al. (54) was constructed: a truncated version, plasmid pCB84b, in which effectively the upstream nucleosome and UASpA and UASpB were deleted ($\Delta\Delta$ UASpAB [schematic in Fig. 3A]), and point mutants for either one of the Pho4 binding sites, UASpC, UASpD, and UASpE, or for two sites together, i.e., UASpCEmut or UASpDEmut. For the truncated promoter the proper positioning of the downstream nucleosome in the repressed state and the generation of the corresponding extended hypersensitive region (truncated eHS type) upon induction were confirmed by DNase I indirect end labeling (data not shown).

Induction of the truncated promoter $\Delta\Delta$ UASpAB as monitored by acid phosphatase activity was very similar to the wt promoter (Fig. 3A). Mutation of the accessible high-affinity sites, UASpC or UASpD, affected the final promoter activity rather slightly, with the effect of the UASpD mutation being a bit more pronounced (Fig. 3A). In contrast, the absence of the intranucleosomal low-affinity site, UASpE, had a much stronger effect, reducing the final promoter strength by more than 50%. The combination of mutations in the UASpE and either UASpC or UASpD sites drastically reduced the final promoter activity to about 25% and 15% of the wt activity, respectively. We conclude, in agreement with Ogawa et al. (54), that the contribution of UASpC and UASpD was redundant, whereas UASpE contributed about half the promoter activity by itself. Further, there was some cooperativity between the intranucleosomal UASpE site and the accessible site UASpD and maybe also UASpC, as the effects of the double mutants were larger than the sum of the effects of each single mutant.

Next we examined if the effects on promoter strength were a consequence of inefficient promoter chromatin remodeling or of an effect downstream of chromatin opening. The DNase I indirect end-labeling patterns under inducing conditions of the UASpCmut or UASpDmut promoter variants were the same as for the wt promoter (data not shown), which was in agreement with a rather slight effect of these mutations on promoter activity. The finding that one UASp element in the sHS linker was sufficient for full remodeling of the upstream and downstream nucleosome is similar to the *PHO8* but different from the *PHO5* promoter, where the linker site UASp1 alone was not sufficient for chromatin remodeling (25). This may be because UASp1 at the *PHO5* promoter is a low-affinity binding site, in contrast to the high-affinity linker sites at the *PHO84* and *PHO8* promoters (5, 7, 54).

Any promoter variant lacking UASpE showed a hypersensitive region under inducing conditions that was less extensive in the downstream direction (eHS*) (Fig. 3C, schematic). This was especially clear in the DNase I patterns of the induced UASpCEmut and UASpDEmut promoter variants (Fig. 3C and data not shown), in which the extended hypersensitive region (eHS*) extended only up to about the SpeI marker band (-259 bp) (Fig. 3C), which was introduced with the UASpEmut point mutation and marked therefore the position

of UASpE. In contrast, the eHS region of the induced wt promoter pattern reached further downstream beyond the AgeI marker (bp -172) (Fig. 1A and B and 3B). This less-extensive eHS* region was less clearly visible in the DNase I pattern of the UASpEmut variant (Fig. 3C), but less extensive remodeling downstream of the SpeI site was confirmed also for this variant by a reduced final accessibility of the AgeI site (Fig. 3C, table). We concluded that UASpE is essentially required for remodeling of the region between the downstream nucleosome and the TATA box.

Gcn5 is not essential for *PHO84* promoter remodeling, but its absence causes a strong delay in histone eviction kinetics and concomitant promoter induction. Previously, we found that remodeling of the chromatin structure at the weak *PHO8* promoter was critically dependent on Gcn5 and Snf2 (28). At the stronger *PHO5* promoter only the rate of chromatin remodeling was strongly decreased in the absence of Gcn5 or Snf2 (6, 8, 19), but eventually full remodeling was achieved. We wondered if remodeling at the even stronger *PHO84* promoter would be mostly or even fully independent of the presence of these cofactors.

First, we examined induction kinetics of the *PHO84* promoter in *gcn5* cells and found a strong delay in comparison to wt cells, even though the final induction level was unaffected (Fig. 4A). In agreement with this, the DNase I pattern of the fully induced promoter in the *gcn5* mutant was the same as observed in wt cells (Fig. 4B). Therefore, the Gcn5 activity had no essential role for the final opening of the *PHO84* promoter chromatin. This was confirmed further by restriction enzyme analysis of DNA accessibility at the entire promoter region under fully inducing conditions (Fig. 4C and D, $-P_i$).

In analogy to our earlier findings at the *PHO5* promoter (8), we assumed that the kinetic delay on the activity level in the *gcn5* mutant (Fig. 4A) was caused by a delay in the chromatin remodeling step. We quantified chromatin opening for wt and *gcn5* cells by restriction enzyme accessibility at 1.5 h after shift to phosphate-free medium and by histone H3 ChIP during an induction time course. To our surprise, we did not catch much of a delay in the increase of restriction enzyme accessibility at this time point of induction. There was only a slight delay compared to wt in opening at the AgeI site, i.e., in the region between the downstream nucleosome and the TATA box (Fig. 4C and D, 1.5 h, $-P_i$). For comparison, chromatin remodeling at the *PHO5* promoter, as probed by ClaI accessibility, was still strongly delayed after 3 hours of induction in a *gcn5* strain (8). Nonetheless, we did observe a strong delay in histone eviction kinetics as monitored by histone H3 ChIP (Fig. 4E). Even after 2 hours of induction, there was six to seven times more histone H3 still present at the promoter in the *gcn5* mutant than in the wt cells. Therefore, we observed for the first time a large disparity between restriction enzyme accessibility and histone H3 eviction kinetics during induction of a PHO promoter. We conclude that histone eviction, rather than an initial increase of DNA accessibility, appeared to be the rate-limiting step in *PHO84* promoter opening in a *gcn5* mutant.

In the absence of Snf2, remodeling of the *PHO84* promoter chromatin structure is only partial: the downstream nucleosome is fully remodeled but the upstream one is not at all. Second, we examined *PHO84* promoter induction kinetics in a *snf2* mutant and observed a similar delay as with the *gcn5*

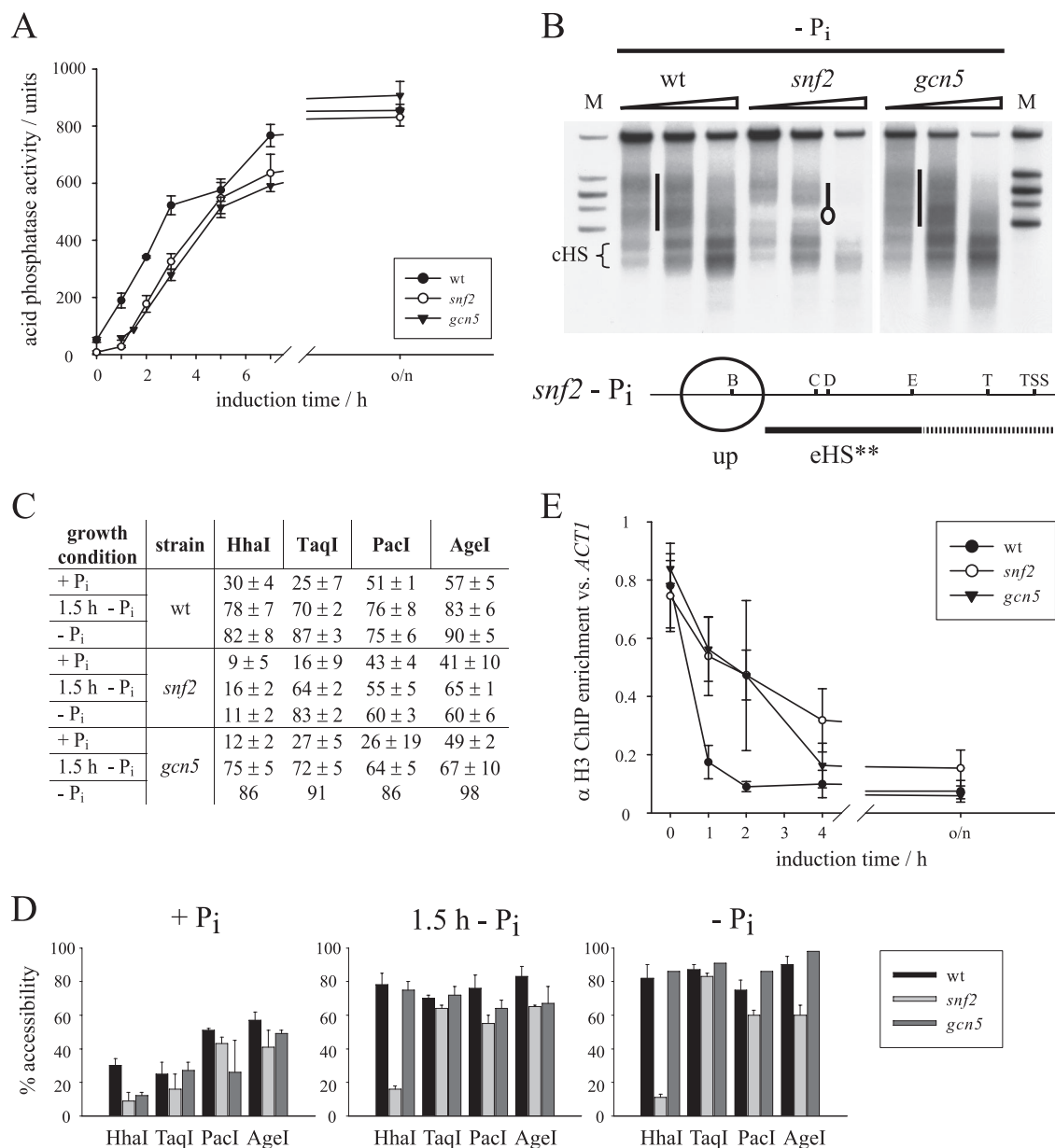


FIG. 4. Chromatin remodeling at the *PHO84* promoter is incomplete and delayed in the absence of Snf2 and only delayed in the absence of Gcn5. (A) *PHO84* promoter induction kinetics as in Fig. 3A for wt (CY339 pCB84a), *snf2* (CY409 pCB84a), and *gcn5* (CY53379 *pho5* pCB84a) strains. o/n, overnight induction. (B) DNase I indirect end-labeling analysis of the *PHO84* promoter chromatin structure at the chromosomal locus in the induced state ($-P_i$) for wt (CY339 pCB84a-UASpCEmut), *snf2* (CY409 pCB84a-UASpCEmut), and *gcn5* (CY53379 *pho5* pCB84a) strains. Marker lanes (M) are as described for Fig. 1A (AgeI, MfeI, ApaI, and BsrBI, from top to bottom). The vertical bars between the second and third and between the eighth and ninth lanes mark the eHS (as in Fig. 1A) of the induced wt promoter pattern. The bar and oval between the sixth and seventh lanes corresponds to the schematic below the blot that illustrates the semiremodeled pattern of the induced *PHO84* promoter in a *snf2* strain. eHS** denotes the reduced extended hypersensitive region of this pattern. All other labeling is analogous to that for Fig. 1A and B. All samples were electrophoresed in the same gel, but for the *gcn5* data a stronger exposure is shown. (C) Average accessibility values for the indicated restriction enzymes under conditions of repression ($+P_i$), full induction ($-P_i$), and an early time point of induction (1.5 h $-P_i$) for wt, *snf2* (CY409 pCB84a), and *gcn5* (CY53379 *pho5* pCB84a) strains. The wt $+P_i$ and $-P_i$ data are the same as in Fig. 1D, and the wt 1.5-h $-P_i$ data were generated with strain CY339 pCB84a. Averages are derived from two to four biological replicates if a variation is given. (D) Same data as shown in panel C, but plotted as bar diagrams and grouped according to growth conditions. (E) Histone loss kinetics as in Fig. 2 using the *PHO84* promoter amplicon with wt (CY337), *snf2* (CY407), and *gcn5* (CY53379) strains. Error bars show the standard deviations of three biological replicates. o/n, overnight induction.

mutant, again with hardly any effect on the final level of induction (Fig. 4A). In marked contrast and much to our surprise, this final activity of the *snf2* strain corresponded to an only partially open DNase I pattern of the induced *PHO84*

promoter, both on the chromosomal and the plasmid locus (Fig. 4B and data not shown). The downstream nucleosome was remodeled, but the upstream one was not at all. In addition, we noticed that the spreading of the eHS region was less

extensive in the downstream direction than in the wt case (eHS**) (Fig. 4B, schematic) and confirmed this by a reduced final accessibility of the AgeI and PacI sites (Fig. 4C and D, $-P_i$). This reduced downstream spreading of the eHS** region was similar to the reduced spreading of the eHS* region in the UASpEmut variant (Fig. 3C). It was even somewhat more severe, as also the PacI site accessibility was reduced in the eHS** but not in the eHS* region (Fig. 4C and 3C, tables). Even though the eHS** region in the *snf2* mutant was less remodeled than the eHS* region in the UASpEmut variant, it was still compatible with full final activity levels (Fig. 4A). So, we concluded that the lower final activity in the UASpEmut, and even more so in the UASpCEmut and UASpDEmut variants (Fig. 3A), was less due to compromised chromatin remodeling but mainly due to the reduced number of UASp elements (see also reference 41). As the transition from the semiopen to the fully open state in the region between the downstream nucleosome and the TATA box was compromised in both the *snf2* mutant and the UASpEmut variant, we suggest that recruitment of the SWI/SNF complex by UASpE-bound Pho4 was essential for chromatin remodeling in this region.

Restriction enzyme probing of the induced state in the *snf2* mutant also confirmed the lack of remodeling of the upstream nucleosome, i.e., persistently low HhaI accessibility, and full remodeling of the downstream nucleosome, i.e., high TaqI accessibility (Fig. 4C and D, $-P_i$). Altogether, this chromatin pattern constituted a third type of extended hypersensitive region (eHS**) (Fig. 4B, schematic), where the upstream nucleosome was still present, the downstream nucleosome fully remodeled, and the region between the downstream nucleosome and the TATA box not fully remodeled.

The same partially remodeled DNase I pattern was also observed in the *snf2K798A* strain, which bears a point mutation in the Snf2 ATPase domain (Fig. 5A), confirming that the ATPase activity of Snf2 rather than some other feature of the SWI/SNF complex was responsible for the observed effect.

In analogy to the *gcn5* mutant, we examined whether the kinetic delay of *PHO84* promoter induction in the *snf2* mutant (Fig. 4A) corresponded not only to the aforementioned reduction in the final extent of remodeling but also to a kinetic delay of chromatin opening, for example, at the TaqI site in the downstream nucleosome. After 1.5 h of induction there was not much delay in opening of the TaqI or any other site, based on the 1.5-h values for the *snf2* strain compared to wt and normalized to their respective $-P_i$ values (Fig. 4C and D). However, histone eviction kinetics measured by histone H3 ChIP in *snf2* cells showed a strong delay (Fig. 4E). At present we are unsure why the final level of histone occupancy at the induced *PHO84* promoter in *snf2* cells as measured by histone H3 ChIP was not much higher than for the wt and *gcn5* strains. This would be expected due to the continued presence of the upstream nucleosome in the *snf2* strain. The resolution of our ChIP analysis (about 500 bp) cannot distinguish between the upstream and the downstream nucleosome, because the amplicon used (Fig. 2, schematic) will score fragments from both nucleosome regions. However, as the upstream nucleosome was not remodeled at all and as the downstream region close to the TATA box was remodeled to a lesser extent than in the wt (see above), we assume that histone H3 ChIP mainly monitored remodeling of the downstream nucleosome. Therefore,

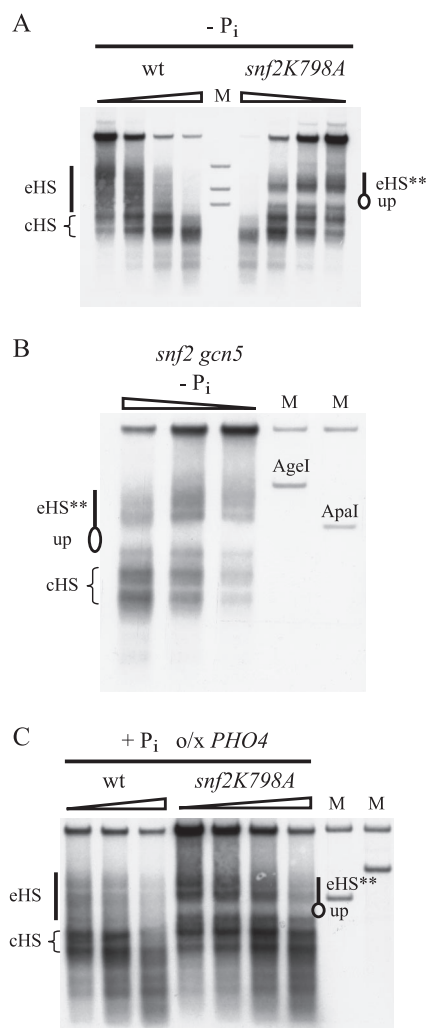


FIG. 5. The Snf2 ATPase domain point mutant as well as a *snf2 gcn5* double mutant show the same *PHO84* promoter chromatin organization in the induced state as the *snf2* deletion mutant. (A) DNase I indirect end labeling of the induced *PHO84* promoter chromatin structure in wt (CY396) and *snf2K798A* (CY397) strains. Labeling is analogous to that used in Fig. 1A and 4B. Marker fragments (lane M) correspond to double digests with HindIII and either AgeI, ApaI, or BsrBI (from top to bottom in the lane). (B) DNase I indirect end labeling of the induced *PHO84* promoter chromatin structure in a *snf2 gcn5* strain (FY1352). Labeling is as for panel A. Marker fragments correspond to double digests with HindIII/AgeI (left lane M) and HindIII/ApaI (right lane M). (C) DNase I indirect end labeling of the *PHO84* promoter chromatin structure under conditions of *PHO4* overexpression (*o/x PHO4*) in phosphate-containing medium ($+P_i$) for wt (CY396 pP4-70I) and *snf2K798A* (CY397 pP4-70I) strains. Labeling is as for panel A. Marker fragments correspond to double digests with HindIII/ApaI (left lane M) and HindIII/AgeI (right lane M).

the delayed histone eviction in the *snf2* mutant argues for a role of Snf2 in remodeling of the downstream nucleosome. Similar to the case of the *gcn5* mutant, also here histone eviction seemed to be the rate-limiting step.

As remodeling of the downstream nucleosome was eventually complete but kinetically delayed at the histone eviction step in both the *snf2* and *gcn5* single mutants, we wondered if the downstream nucleosome may not open up at all in a *snf2*

gcn5 double mutant. This was not the case, as the DNase I pattern of the fully induced *PHO84* promoter in the *snf2 gcn5* double mutant was indistinguishable from that found in *snf2* cells (Fig. 5B).

Previously, it was shown by us and others that submaximal induction conditions can exacerbate the dependency of *PHO5* promoter chromatin remodeling on chromatin cofactors (19, 38). Such submaximal induction conditions may be achieved by using low-phosphate rather than phosphate-free medium (19) or by overexpression of Pho4 in high-phosphate medium (25). We tested under the latter conditions whether the differential requirement of Snf2 for remodeling of the downstream and the upstream nucleosome still persisted at submaximal induction. DNase I indirect end-labeling analysis under these submaximal induction conditions showed the same pattern as under fully inducing conditions, for both the wt as well as the *snf2K798A* mutant (Fig. 5C). So, even at such low induction levels the downstream nucleosome could be remodeled without Snf2 activity, demonstrating further the different degree of Snf2 requirement for remodeling of the upstream and downstream nucleosome.

The semiopen chromatin structure close to the TATA box is not sufficient, and basal remodeling of the upstream nucleosome is not necessary for substantial basal *PHO84* transcription. The *pho4*, *snf2*, and *gcn5* mutants all had a decreased basal level of transcription (Fig. 4A and data not shown) (69). In all these three mutants the semiopen less-organized chromatin structure between the downstream nucleosome and the TATA box was not affected in the repressed state. Therefore, this semiopen structure was not sufficient for sustaining substantial basal transcription under repressing conditions.

Nonetheless, in all three mutants the accessibility of the HhaI site under repressing conditions was reduced in comparison to wt, in *snf2* and *gcn5* cells even more so than in the *pho4* mutant (Fig. 4C and D, +P_i, and 1D, table). The reduced HhaI accessibility might have been responsible for the reduced basal transcription. In the wt, the targeted recruitment of Snf2 and Gcn5 by Pho4 could keep the upstream nucleosome in a partially remodeled state, which would allow partial access to UASpB and lead to even more remodeling of the upstream nucleosome and high basal transcription. To test this, we introduced a point mutation in UASpB and found indeed that the HhaI site accessibility under +P_i conditions (19 ± 2%) was significantly lower than at the wt promoter and similar to that of the wt promoter in the *pho4* mutant (17 ± 2%) (Fig. 1D). However, despite this lower HhaI accessibility there was hardly any effect on the basal level of activity for the UASpBmut construct (data not shown), arguing that UASpB and basal remodeling of the upstream nucleosome were not necessary for the substantial basal transcription. In addition, mutation of the other intranucleosomal site, UASpE, which analogously may have been involved in basal remodeling of the downstream nucleosome, did not affect basal transcription either (Fig. 3A).

Ino80 is not essential for chromatin opening at the entire *PHO84* promoter, neither in wt nor in *snf2* cells, but its absence causes a strong delay in chromatin opening kinetics. As we had already observed a cooperation between Snf2 and Ino80 for chromatin remodeling at the *PHO5* and *PHO8* promoters (6), and as others have shown a recruitment of both

Snf2 and Ino80 to the *PHO84* promoter upon induction (23, 36, 72), we investigated the role of Ino80 for *PHO84* promoter opening. In particular, there was the possibility that Ino80 would be the alternative remodeler for remodeling of the downstream nucleosome in the absence of Snf2.

The absence of Ino80 by itself did not prevent full remodeling of the *PHO84* promoter chromatin structure, i.e., the DNase I pattern of an *ino80* mutant under fully inducing conditions corresponded to the eHS type of the wt (Fig. 6A) and the accessibility of restriction enzymes along the promoter region increased to almost-wt levels (Fig. 6C). Further, the DNase I pattern of the induced promoter in the *snf2 ino80* double mutant was indistinguishable from the pattern of the *snf2* single mutant (Fig. 6B). Together, these results argue that Ino80 was neither essentially required for remodeling under fully inducing conditions in the wt strain nor for remodeling of the downstream nucleosome in the absence of Snf2. Nonetheless, the chromatin opening kinetics in the *ino80* strain was strongly delayed over the entire promoter region after 1.5 h of induction as examined by restriction enzyme accessibility (Fig. 6C). Therefore, Ino80 is clearly involved in the wt chromatin remodeling pathway at the *PHO84* promoter.

In contrast to Snf2 and Gcn5, Ino80 was not involved in keeping the upstream nucleosome in a partially remodeled state under repressing conditions (+P_i), as the HhaI accessibility was not affected in the *ino80* mutant (Fig. 6C, table, +P_i). A slight decrease in PacI accessibility may indicate that Ino80 has a minor role in positioning the downstream nucleosome under repressing conditions.

As presented above for the case of Snf2, we checked if *PHO84* promoter opening became more dependent on Ino80 under submaximal conditions. Strikingly, the DNase I patterns of the *snf2K798A* and the *ino80* mutants at submaximal induction were indistinguishable, i.e., under these conditions the upstream nucleosome became strictly dependent also on Ino80 (Fig. 6D).

The stricter cofactor requirements for remodeling of the upstream nucleosome correlates with higher intrinsic stability as measured in vitro and predicted in silico. As shown above, remodeling of the upstream nucleosome was strictly dependent on Snf2, whereas remodeling of the downstream nucleosome was not (Fig. 4B and 5A). In addition, remodeling of the upstream nucleosome was more dependent on Ino80 than remodeling of the downstream nucleosome (Fig. 6D). This constitutes a case of differential cofactor requirements for nucleosome remodeling within one and the same promoter.

We found earlier that the differential cofactor requirements for chromatin remodeling at the *PHO5* and *PHO8* promoters correlated with differential intrinsic stabilities of the positioned nucleosomes (31). These stabilities were measured using our yeast extract chromatin assembly system that is able to generate the proper in vivo nucleosome positioning de novo in vitro (31, 39). In this system, plasmids bearing the yeast locus of interest are assembled by salt gradient dialysis into a chromatin structure with a specific but usually not proper, i.e., not in vivo-like, nucleosome positioning pattern. The in vivo-like pattern is induced in the next step by the addition of yeast whole-cell extract in the presence of energy. A so-far-unidentified energy-dependent activity in the yeast extract apparently constitutes the thermodynamic conditions for in vivo-like nucleo-

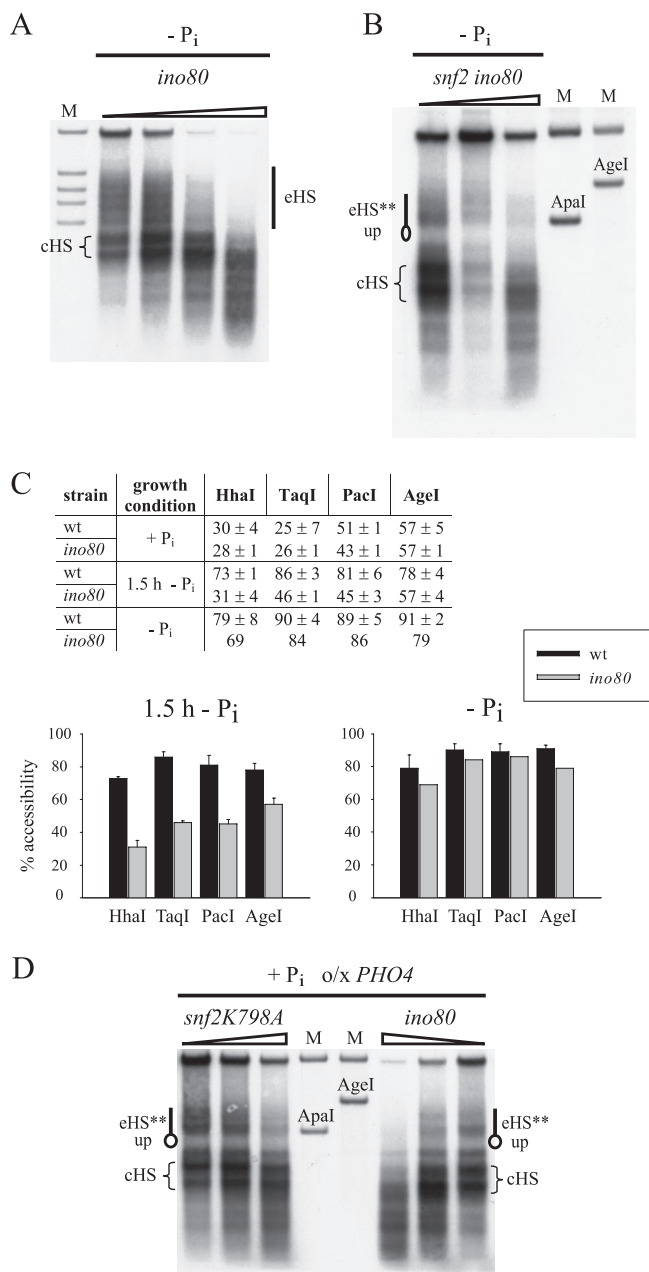


FIG. 6. Chromatin remodeling at the *PHO84* promoter is delayed in the absence of Ino80. (A) DNase I indirect end-labeling analysis of the induced *PHO84* promoter chromatin structure for an *ino80* strain (BY4741-1). Labeling is as for Fig. 1A and 4B. Marker in lane M is as in Fig. 1A (AgeI, MfeI, ApaI, and BsrBI, from top to bottom). (B) DNase I mapping as for panel A, but for the *snf2 ino80* double mutant (CY407 *ino80*). Marker fragments correspond to double digests with HindIII/ApaI (left lane M) and HindIII/AgeI (right lane M). Labeling is as for Fig. 1A and 5B. (C) Restriction enzyme accessibility data are as for Fig. 4C and D for wt (BY4741) and *ino80* (BY4741-1) strains. Averages are derived from two to three biological replicates if a variation is given. The wt + Pi data are the same as those in Fig. 1D. (D) DNase I mapping of the *PHO84* promoter under submaximal induction conditions as in Fig. 5C for *snf2K798A* (CY397 pP4-70I) and *ino80* (BY4741-1 pP4-70I) strains. The left five lanes are the same as the right five lanes in Fig. 5C. Labeling and markers as in Fig. 5C.

some positioning. In a next step, it is possible to compare the intrinsic stability of properly positioned nucleosomes by titrating the histone concentration. Under conditions of limiting histones (underassembled chromatin) there are fewer nucleosomes deposited onto the DNA than there are nucleosome positions available. Therefore, the multitude of alternative and mostly overlapping nucleosome positions will compete for nucleosome occupancy. Positions that are already occupied in equilibrium in underassembled chromatin are more stable than those that are occupied only in fully assembled chromatin (for a full discussion of this methodology see reference 31). Using this approach, we observed previously that the proper positioning over the *PHO5* promoter region could only be generated in fully assembled chromatin, whereas the proper *PHO8* promoter pattern was also achieved in underassembled chromatin. Therefore, the intrinsic stability of the *PHO8* promoter nucleosomes was higher than the stability of the *PHO5* promoter nucleosomes.

With the same methodology we compared the intrinsic stability of the upstream and downstream nucleosome at the *PHO84* promoter (Fig. 7A and B). First, we prepared fully assembled salt gradient dialysis chromatin (histone octamer:DNA mass ratio set as 100%) using a plasmid with a 3.5-kb *PHO84* insert as template and tested if the yeast extract would generate the in vivo pattern. Much to our surprise, we observed that the DNase I pattern of the salt gradient dialysis chromatin was already very similar to the in vivo pattern (Fig. 7A, compare SGD and in vivo). This pattern was clearly different from a digest of free DNA and did not change much, as expected (31), with the addition of yeast extract in the absence of energy. This was the first case out of 14 tested yeast loci (C. Wippo and P. Korber, unpublished results) where salt gradient dialysis by itself was already able to generate a very in vivo-like chromatin structure. This suggests that rather strong nucleosome positioning sequence elements in the *PHO84* promoter lead to in vivo-like nucleosome positioning already under pure salt gradient dialysis conditions. Nonetheless, incubation with yeast extract and energy did make the pattern more similar to the in vivo pattern, especially regarding the relative band intensities and the upper part of the lane, i.e., the coding region (Fig. 7A, compare SGD + Yex/ATP with in vivo). Therefore, the *PHO84* promoter is one more example where our yeast extract in vitro assembly system constitutes conditions more similar to in vivo conditions for nucleosome positioning than salt gradient dialysis alone.

Second, we repeated the salt gradient dialysis chromatin assembly with limiting histones (histone octamer:DNA mass ratio of 60%) and still obtained a rather in vivo-like pattern (Fig. 7B). This in vivo-like pattern again did not change upon the addition of yeast extract without energy. However, incubation with yeast extract in the presence of energy, i.e., conditions that should be closer to the in vivo conditions, had a differential effect on the regions upstream and downstream of the sHS region. The upstream nucleosome and the cHS region again became even more like the in vivo pattern, but the sHS region was so much extended further downstream that the position of the downstream nucleosome was compromised. The sHS region was always somewhat sharper in the pure salt gradient dialysis chromatin pattern and became fuzzier upon addition of yeast extract and energy, also with fully assembled chroma-

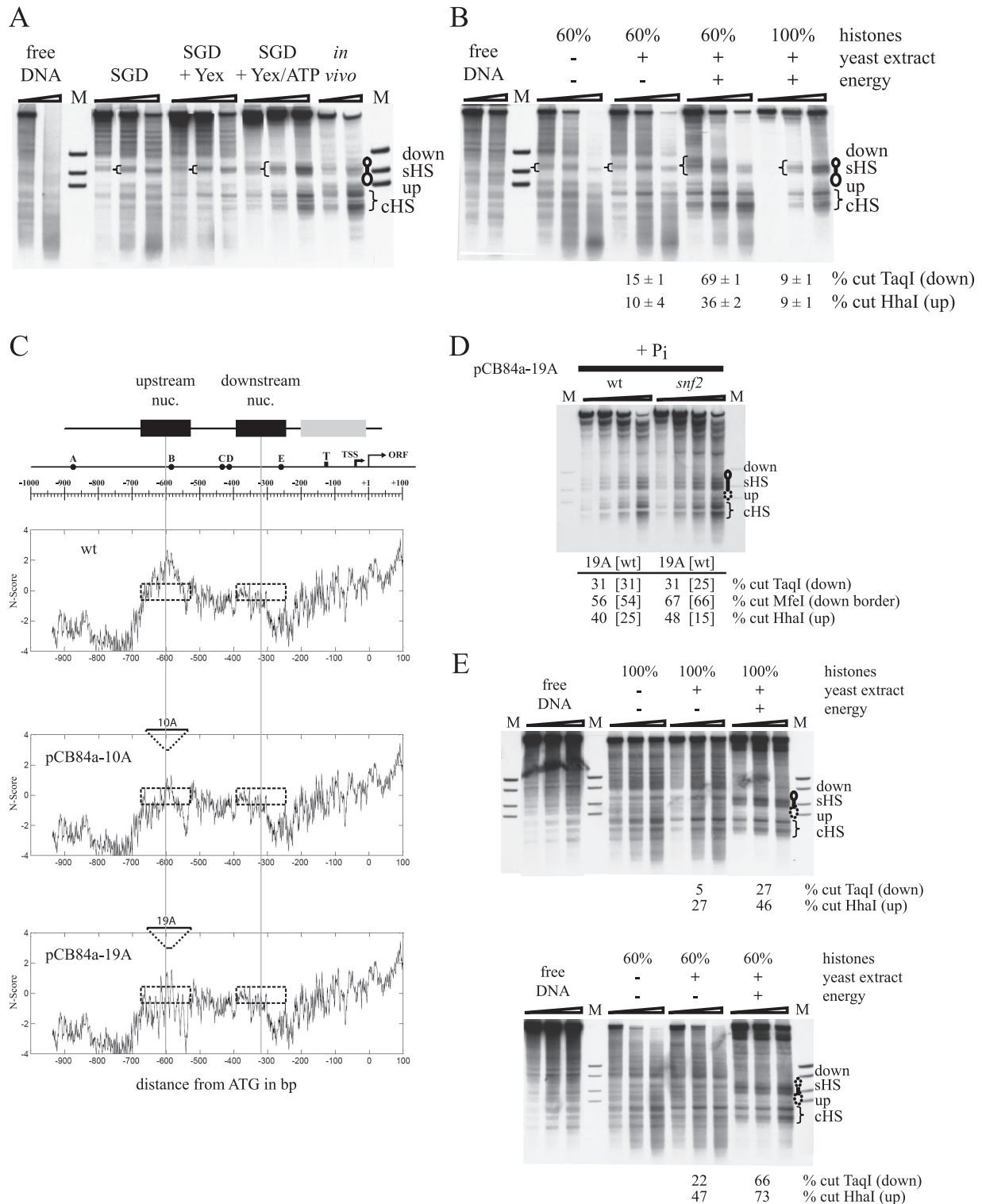


FIG. 7. The nucleosome upstream of the short hypersensitive site at the *PHO84* promoter has higher intrinsic stability than the downstream nucleosome and can be destabilized by introducing poly(dA) stretches. (A) DNase I indirect end-labeling analysis of the *PHO84* promoter region on plasmid pUC19-*PHO84* in vitro either as free DNA or after chromatin assembly by salt gradient dialysis (SGD) and further incubation with yeast extract in the absence (SGD + Yex) or presence of energy (SGD + Yex/ATP). The *PHO84* promoter chromatin pattern of the repressed state in vivo is shown for comparison. Marker fragments (lanes M) correspond to double digests with *SspI* and either *AgeI*, *ApaI*, or *BsrBI* (from top to bottom in the lanes). Schematics next to the blot are as described for Fig. 1A. Brackets in the lanes highlight the extent of the sHS region. (B) DNase I indirect end-labeling and markers (lane M) as for panel A but with either underassembled (60% histones) or fully assembled (100% histones); the same degree of assembly as in panel A) salt gradient dialysis chromatin on plasmid pUC19-*PHO84* and incubation with yeast extract and energy as indicated. Brackets in the lanes mark the extent of the sHS under the different chromatin assembly conditions. The accessibilities

tin templates (Fig. 7A; compare widths of brackets). But whereas the more fuzzy sHS region in the fully assembled chromatin (100%) resembled more the *in vivo* case, it was stretched too far downstream to be compatible with a proper positioning of the downstream nucleosome for the underassembled chromatin templates (60%) (Fig. 7B; compare widths of brackets). We stress that the more extensive sHS region under underassembled conditions compared to fully assembled conditions (Fig. 7B) was not due to the use of different degrees of DNase I digestion, as we saw such a difference significantly and repeatedly over a wider range of DNase I digestions (data not shown).

This differential effect on the upstream and downstream nucleosome was confirmed by restriction enzyme accessibility assays. The accessibility of the TaqI site in the downstream nucleosome increased much more (from 15% to 69%) (Fig. 7B) upon addition of extract and energy to underassembled chromatin than the accessibility of the HhaI site in the upstream nucleosome (from 10% to 36%). The overall lower accessibilities in the fully assembled chromatin compared to the *in vivo* situation probably reflected here a subpopulation of aggregated, i.e., indigestible, templates *in vitro*, which may form especially at such high histone concentration. Altogether, these results suggested that the downstream nucleosome was intrinsically less stably positioned *in vivo* than the upstream nucleosome. This correlated with its more relaxed cofactor requirements.

The finding of higher intrinsic stability of the upstream nucleosome also correlated strikingly with the prediction of the *N*-score algorithm (84) (Fig. 7C). The *N*-score algorithm was trained on *in vivo* yeast nucleosome positioning data and used to predict the probability for nucleosome occupancy (positive values) or depletion (negative values) rather than exact positions. It showed a positive peak right in the middle of the upstream nucleosome, maybe suggesting an especially stable nucleosome here *in vivo*. In contrast, the DNA sequence underlying the downstream nucleosome was rather neutral, or even negative at its 3' end, with regard to the propensity for nucleosome occupancy.

Introduction of destabilizing mutations into the DNA sequence of the upstream nucleosome relieves the *Snf2* dependency for its remodeling *in vivo*. So far, we correlated, in this

and our previous study (31), intrinsic nucleosome stability and the cofactor requirement. Next we wished to test directly if stability was causative for requirement. Extended stretches of poly(dA-dT) are known to be unfavorable for nucleosome formation *in vivo* and *in vitro* (4, 33, 57). So we replaced a stretch of 10 or 19 consecutive bases with adenine deoxynucleotides (plasmids pCB84a-10A and -19A, respectively) in the middle of the upstream nucleosome region (Fig. 7C). As expected, such replacements led to increasingly more negative *N*-scores for the region that was occupied by the upstream nucleosome in the wt promoter (Fig. 7C).

We needed to check if the upstream nucleosome would still form *in vivo* on these mutated DNA templates. DNase I mapping confirmed the presence of the upstream nucleosome for both variants in the wt and *snf2* backgrounds (Fig. 7D and data not shown). Restriction enzyme accessibility assays showed that there was no increase in HhaI site accessibility for the 10A replacement compared to the wt promoter (data not shown) but an increase for the 19A variant (from 25 to 40% in wt and from 15 to 48% in the *snf2* background) was observed (Fig. 7D). This suggested a destabilized upstream nucleosome for the 19A variant already under repressive conditions. There was also a subtle shift in positioning as the sHS region extended more upstream beyond the ApaI marker (compare Fig. 7D and 3B). This region of additional hypersensitivity at the 3' border of the upstream nucleosome correlated with the region of the most negative *N*-score at about -550 (Fig. 7C).

The reduced stability of the 19A variant was directly assessed in our *in vitro* chromatin assembly assay (Fig. 7E). First, the upstream nucleosome formed neither with a limiting (60%) nor with the full (100%) complement of histones during salt gradient dialysis, but the DNase I pattern in this region was similar to that of the free DNA digest. This speaks for the lower nucleosome positioning power of the mutated DNA sequence under these conditions. Second, the addition of yeast extract and energy induced a more *in vivo*-like chromatin structure in the fully assembled (100%) chromatin template, with accessibilities for the HhaI and TaqI sites that were very similar to the *in vivo* values (Fig. 7D and E; compare 19A in the wt background [D] and 100% with yeast extract and energy [E]). This confirmed again that the unidentified energy-dependen-

of the respective chromatin states to HhaI and TaqI (monitoring the accessibility of the upstream and downstream nucleosome, respectively, by the same assay as shown in Fig. 1C) are given underneath the blot. Average values and variations are derived from two independent treatments of a given salt gradient dialysis chromatin preparation. DNase I mapping data were reproduced with two independent salt gradient chromatin preparations. (C) The scheme on top shows the *PHO84* promoter chromatin organization, with black boxes indicating the positioned upstream and downstream nucleosomes and the gray box representing the less-organized structure close to the TATA box. The positions of five UASp elements (A to E), of the TATA box (T), transcription start site (TSS), and the ORF are indicated on top of the scale that plots the distance in base pairs from the ATG (+1). The three graphs show the *N*-score (84) plotted against the distance from the ATG in base pairs for the wt *PHO84* promoter and for promoter variants where stretches of 10 or 19 bases were replaced with homopolymeric deoxyadenylate at the indicated positions in the plasmids pCB84a-10A and pCB84a-19A, respectively. Stippled boxes show the positions of the upstream and downstream nucleosomes as in the schematic above, and thin gray lines mark the center of these nucleosomes. (D) DNase I indirect end-labeling analysis of the *PHO84* promoter chromatin structure at the plasmid locus in wt (CY339 pCB84a-19A) and *snf2* (CY409 pCB84a-19A) strains under repressive conditions (+P_i). Markers (lanes M) are as for panels A and B (AgeI, ApaI, and BsrBI, from top to bottom). Labeling is as in Fig. 1A, but the oval representing the upstream nucleosome in the *snf2* strain is stippled to indicate the partially open state. Accessibilities for the indicated restriction enzymes are indicated underneath the blot, as for panel B. MfeI monitors the border of the downstream nucleosome toward the sHS region (down border). Values in brackets show the respective accessibilities of the endogenous chromosomal wt promoter in the same cells. (E) DNase I indirect end-labeling and restriction enzyme accessibility assays analogous to those in panel B but with plasmid pUC19-PHO84-19A. Stippled ovals in the schematics indicate destabilized nucleosomes. Marker fragments (M lanes) correspond to double digests with SspI and either ClaI, AgeI, ApaI, or BsrBI (from top to bottom in the lane). All DNase I indirect end-labeling samples in each panel of the entire figure were electrophoresed on the same gel, but images from different film exposure times were combined using Adobe Photoshop CS2.

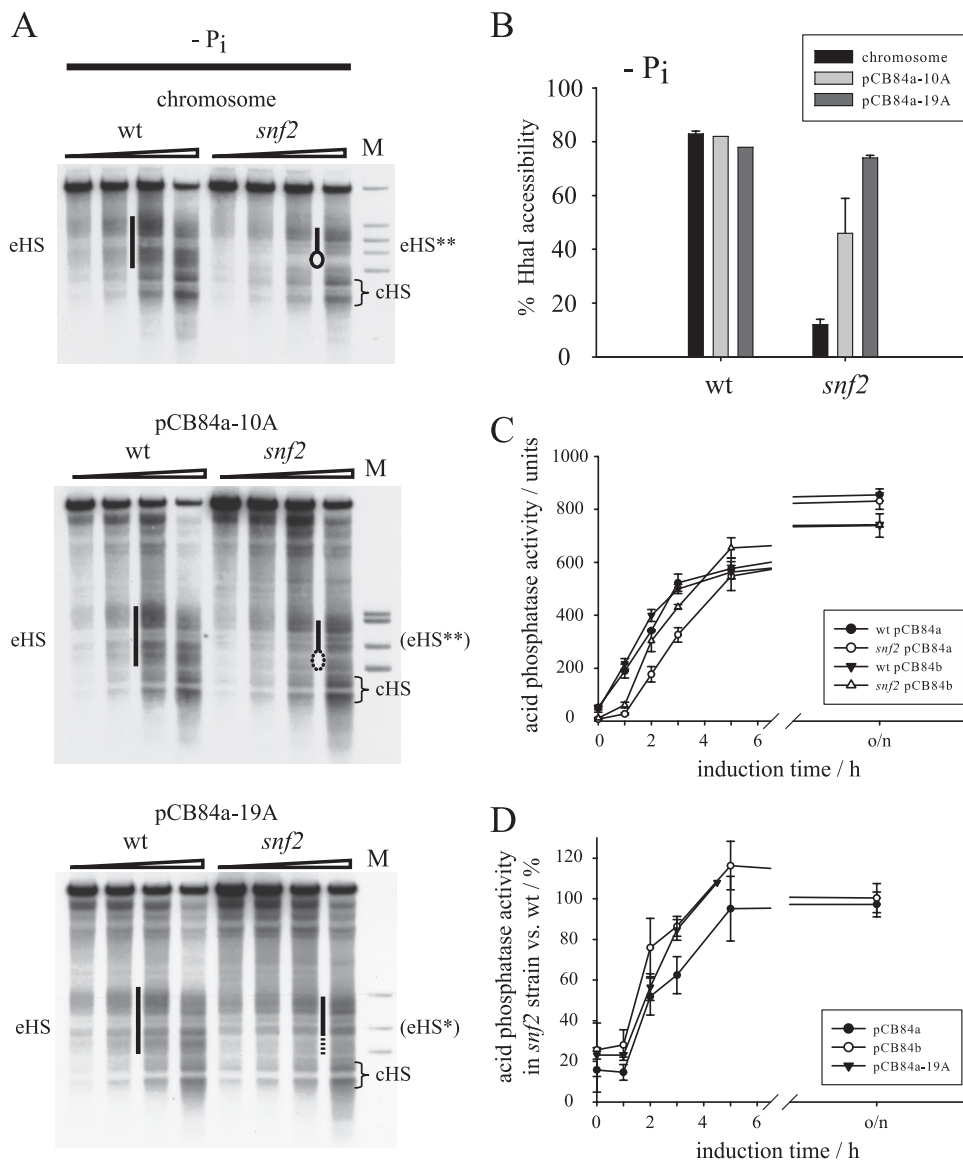


FIG. 8. Mutations that progressively destabilize the upstream nucleosome also progressively relieve its Snf2 dependency of remodeling, but destabilization or complete removal of the upstream nucleosome has only a small effect on the Snf2 dependency of overall promoter induction. (A) DNase I indirect end-labeling analysis as in Fig. 1A for wt (CY339 pCB84a-10A or pCB84a-19A) and *snf2* (CY409 pCB84a-10A or pCB84a-19A) strains under inducing ($-P_i$) conditions, probed for either the chromosomal or the plasmid locus. The top panel shows the chromosomal locus of the strains bearing plasmid pCB84a-10A. The pattern was the same for the strains with plasmid pCB84a-19A (not shown). The middle and bottom panels show the plasmid locus of the indicated plasmids. Labeling is as for Fig. 1A and 5A, but (eHS**) stands for a somewhat more remodeled eHS** (stippled oval representing a partially remodeled upstream nucleosome), and (eHS*) indicates a somewhat less remodeled eHS* (stippled line denoting a not completely remodeled upstream nucleosome) type of extended hypersensitive region. Marker lane M of the top panel is as in Fig. 1A (AgeI, MfeI, ApaI, and BsrBI, from top to bottom), of the middle panel as in Fig. 3B (AgeI, SpeI, ApaI, and BsrBI, from top to bottom), and of the bottom panel as in Fig. 5A (AgeI, ApaI, and BsrBI, from top to bottom). (B) HhaI accessibility for the conditions shown in panel A. Error bars show the variations of two biological replicates (four replicates in the case of the chromosome locus in the *snf2* background). (C) *PHO84* promoter induction kinetics as in Fig. 3A for wt (CY339) and *snf2* (CY409) strains carrying either a reporter plasmid with the full-length *PHO84* promoter (pCB84a) or with a *PHO84* promoter lacking the upstream nucleosome (pCB84b). o/n, overnight induction. (D) Same data as in panel C and additional data for the *snf2* strain with plasmid pCB84a-19A, normalized at each time point to the values of the wt carrying the same respective plasmid.

dent activity in the yeast extract constitutes conditions for more in vivo-like nucleosome positioning. Third, addition of yeast extract and energy to the underassembled (60%) chromatin templates increased not only the TaqI site accessibility (from 22 to 66%) (Fig. 7E), similar as seen before for the wt promoter (from 15 to 69%) (Fig. 7B) but now also the HhaI site

accessibility (from 47 to 73%). This argued for a low stability of both the upstream and downstream nucleosome.

Finally, both variants showed remodeling of the upstream nucleosome upon induction in a *snf2* strain. The extent of remodeling as judged by DNase I indirect end labeling was substantial for both variants in comparison to the internal

control of the wt promoter at the chromosome locus (Fig. 8A) and to the plasmid locus (data not shown). HhaI site accessibility assays confirmed a partial remodeling for the 10A variant and almost full remodeling for the 19A replacement variant (Fig. 8B). Altogether, these results argue strongly that the intrinsic stability of the upstream nucleosome in the wt promoter caused its strict Snf2 requirement for remodeling.

The destabilization or complete absence of the upstream nucleosome relieves the Snf2 dependency of promoter induction only partially. In addition to the mechanistically interesting relationship between intrinsic stability and Snf2 dependency of remodeling of the upstream nucleosome, we asked further if the critical Snf2 dependency of remodeling the upstream nucleosome was the main cause for the Snf2 effect on overall *PHO84* promoter induction kinetics (Fig. 4A). If so, the kinetic delay in a *snf2* background should be reduced if the upstream nucleosome is destabilized (19A variant, plasmid pCB84a-19A) or absent ($\Delta\Delta$ UASpAB variant, plasmid pCB84b). We followed induction kinetics for both variants in the wt and *snf2* backgrounds by acid phosphatase assay and compared them to the kinetics of the wt promoter in both backgrounds (Fig. 8C and D). For both variants the delay of induction in the *snf2* mutant compared to the wt background was somewhat diminished, more so in the case of the truncated promoter and only very slightly in the case of the mutated promoter. This was more apparent after normalization of the phosphatase activity in the *snf2* strains to the respective activity in the wt background at the same time points (Fig. 8D). Nonetheless, as the delay in the *snf2* strains was still substantial in both cases, we reasoned that there was a significant Snf2 dependency of other parts of the *PHO84* promoter besides the upstream nucleosome. For example, we showed specifically that the kinetics of remodeling the downstream nucleosome was dependent on Snf2, as histone eviction of the wt promoter was delayed in the *snf2* mutant (Fig. 4E) (see above).

Since the HhaI accessibility of the *PHO84* promoter variant in pCB84a-19A was considerably increased under repressive conditions in a *snf2* strain (Fig. 7D) but did not result in a higher basal level of transcription (data not shown), it seemed again (see above) that Snf2 had an effect on basal transcription that was not necessarily linked to basal remodeling of the upstream nucleosome.

The histone acetyltransferase Rtt109 has a role for induction of both the *PHO84* and the *PHO5* promoters. We and others found that the histone chaperone Asf1 is involved in the induction of the coregulated *PHO5* and *PHO8* promoters (1, 38). Recently, several groups reported the critical requirement of Asf1 for the activity of the histone acetyltransferase Rtt109, which acetylates histone H3 at lysine 56 (18, 21, 30, 64, 78). This finding raised the question of whether an involvement of Asf1 reflects its role solely as histone chaperone or rather a role of Rtt109. We checked this for induction of the *PHO5* promoter and observed that the delay in induction was virtually the same in the *asf1* and *rtt109* mutants and that there was no further delay in an *asf1 rtt109* double mutant (Fig. 9A). This argued strongly that Asf1 and Rtt109 function together in the same pathway during *PHO5* induction. We also noted that for both the *asf1* mutant as well as the *rtt109* mutant the basal *PHO5* activity levels were slightly but significantly elevated.

In contrast, induction of *PHO84* was significantly delayed

only in the *rtt109* but hardly at all in the *asf1* mutant (Fig. 9B). The induction delay in the *rtt109* mutant was due to a delay on the level of chromatin remodeling as monitored by restriction enzyme accessibility and histone ChIP assays (Fig. 9C, D, and E). However, the effects were much less severe than those in the *snf2*, *gcn5*, or *ino80* mutants (compare to Fig. 4E and 6C), especially as they were rather limited to an early time of induction (45 min). There was hardly any effect on the level of restriction enzyme accessibilities for the *asf1* mutant, and only at 45 min of induction was there a slight delay in histone eviction. This may constitute a weaker pendant to the effects in the *gcn5* and *snf2* strains, i.e., histone eviction being the rate-limiting step.

There was no differential Rtt109 requirement of the upstream and downstream nucleosome discernible, as the kinetics of restriction enzyme site accessibility were similarly delayed for the HhaI and the TaqI sites in the *rtt109* mutant (Fig. 9C). We also checked the effects of the *asf1* and *rtt109* deletions on induction of the truncated pCB84b construct and got similar results as with the full-length pCB84a plasmid (Fig. 9F), speaking for a role of Rtt109 in remodeling of the downstream nucleosome but not excluding a role for remodeling of the upstream nucleosome as well.

The effects of the *asf1* and *rtt109* deletions on *PHO5* and *PHO84* induction showed some dependency on the strain background. In the BY4741 background, the *rtt109* mutant showed a weaker delay for *PHO5* induction than the *asf1* mutant (data not shown). In the W303 background, the *rtt109* mutant had a similar effect on *PHO84* induction as in the BY4741 background, but here also the *asf1* mutant had an appreciable effect, similar to that of the *rtt109* mutant (data not shown).

It was shown that Rtt109 exists in a complex with another histone chaperone, Vps75 (78); however, the absence of Vps75 caused hardly any effect on *PHO5* and *PHO84* induction (data not shown).

DISCUSSION

The induction of the *PHO84* promoter is coupled to a prominent Pho4-dependent chromatin structure transition. In this study we present a characterization of *PHO84* promoter regulation on the level of chromatin structure. The *PHO84* promoter in its repressed state harbored an sHS region flanked by two positioned nucleosomes (upstream and downstream nucleosome) and a semiopen and less-organized chromatin structure close to the TATA box. This chromatin organization became extensively remodeled upon induction, leading to an extended hypersensitive region of about 500 bp and the eviction of histones.

At the outset of our study no data on the nucleosomal structure of the *PHO84* promoter were available. However, during recent years several groups have undertaken genome-wide nucleosome positioning studies in yeast (45, 49, 67, 82, 85). Very recently, during the preparation of the manuscript, Lam et al. (41) mapped the promoter chromatin structures of PHO regulon genes by tiled PCR amplicons with mononucleosomal DNA as template. Their analysis of the *PHO84* nucleosome organization agrees remarkably well with our mapping (Fig. 10A). Even the less-organized structure between the downstream nucleosome and the TATA box region was reflected by a reduced PCR product peak in this

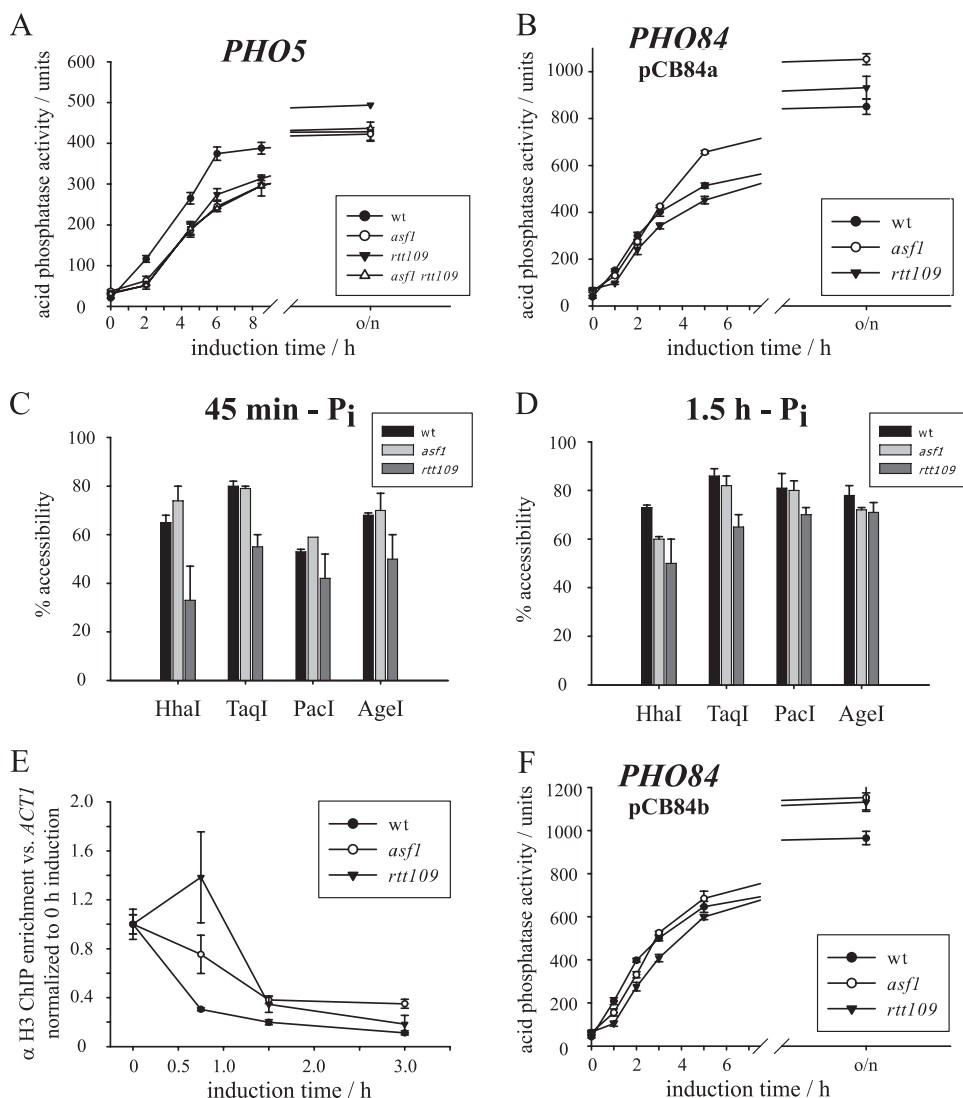


FIG. 9. Induction of the *PHO84* and *PHO5* promoters is delayed in the absence of *Rtt109*, but the effect is weaker for *PHO84* induction and not as pronounced there in an *asf1* strain. (A) *PHO5* promoter induction kinetics as in Fig. 3A but for wt (W303a), *asf1* (W303a *asf1*), *rtt109* (PKY4170), and *asf1 rtt109* (PKY4182) strains. (B) *PHO84* promoter induction kinetics as in panel A for wt (Y00000 pCB84a), *asf1* (Y01310 pCB84a), and *rtt109* (Y01490 pCB84a) strains. (C and D) Restriction enzyme accessibility assays at the chromosomal *PHO84* promoter as in Fig. 1C for the wt (Y00000), *asf1* (Y01310), and *rtt109* (Y01490) strains after 45 min (C) or 1.5 h (D) of induction. Error bars show the variations of two biological replicates. (E) Histone loss kinetics as in Fig. 2 for the same strains as in panels C and D using the *PHO84* promoter amplicon. ChIP data were normalized to input DNA, the *ACT1* amplicon, and to the 0-h values of each strain. Error bars show the variations of two biological replicates. (F) Same experiment as in panel B but with strains carrying plasmid pCB84b.

region. They also found the same extensive nucleosome-free region in the induced state.

In contrast to this congruence of two locus-specific nucleosome mapping studies using different methods, there is less agreement with the genome-wide approaches. The experiments of Lee et al. (45) did not reveal any nucleosomes in the extended *PHO84* promoter region, Whitehouse et al. (82) mapped nucleosomes right in the cHS and sHS regions, and Mavrich et al. (49) correctly assigned the position of the upstream nucleosome and of the cHS and sHS regions but not of the downstream nucleosome. Both our own mapping and that of Lam et al. (41) employed medium with added phosphate to ensure complete repression, whereas the mentioned genome-wide studies used YPD medium, which can

lead to a significant level of *PHO84* transcription (23, 53). These differences in growth conditions could explain at least the lack of nucleosome detection.

We did the analogous comparison of nucleosome positioning data for the *PHO5* and *PHO8* promoter regions and found significant disparities as well, especially for the *PHO8* promoter (Fig. 10B and C). These differences can be less well explained by differences in growth conditions, as both *PHO5* and *PHO8* are largely repressed in YPD medium (3, 5, 53). So, it seems that genome-wide nucleosome positioning data, even though they are extremely valuable for detecting genome-wide trends of nucleosomal organization, may need to be verified by locus-specific mapping techniques.

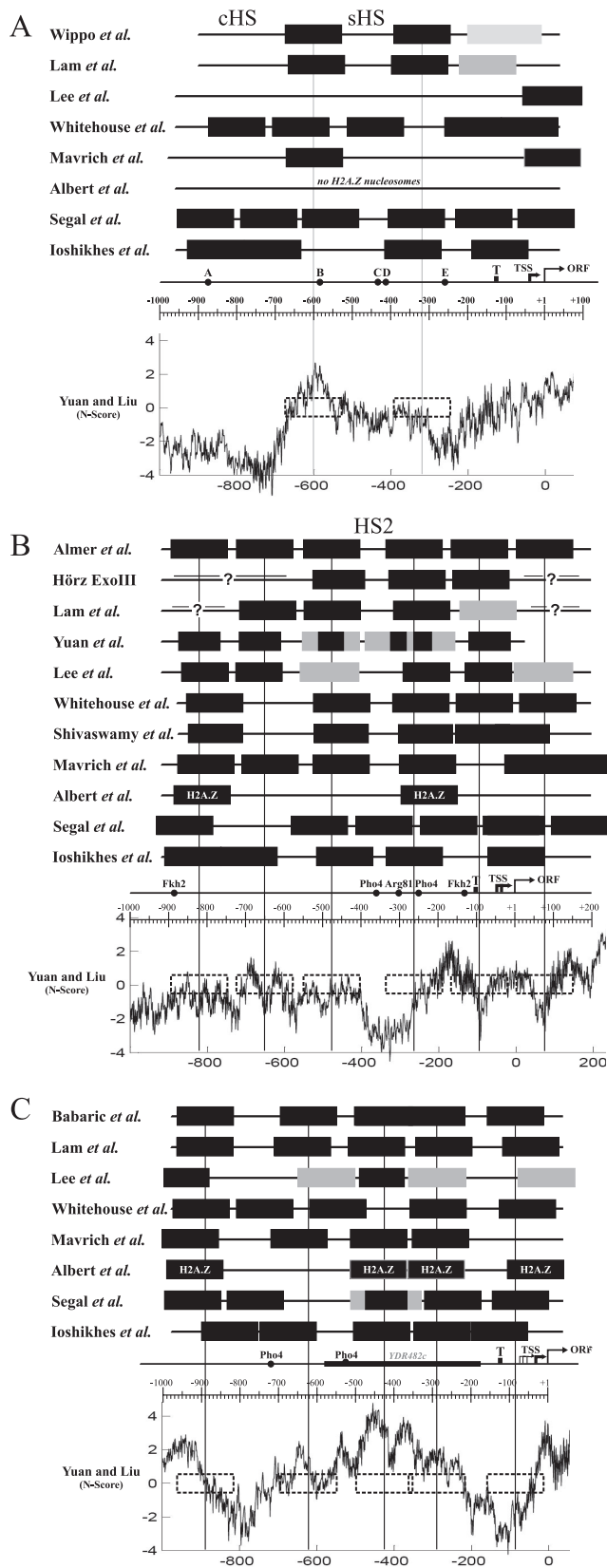


FIG. 10. Comparison of nucleosome positions (filled black rectangles) at the repressed *PHO84* (A), *PHO5* (B), and *PHO8* (C) promoters as measured by (i) individual assays (this study; same positions as in Fig. 1B), Lam *et al.* (41); Almer *et al.* (3); Hörz (unpublished data,

The need for experimental verification is also very important with regard to the prediction of nucleosome positions by DNA sequence-based algorithms. For example, the algorithms of Segal *et al.* (65) and Ioshikhes *et al.* (32) predicted the downstream nucleosome and the extended linker at the sHS region rather well (Fig. 10A). However, the upstream nucleosome was not met and the cHS region was missed. As mentioned above, the *N*-score algorithm of Yuan and Liu (84) accurately predicts low nucleosome occupancy for the cHS region and a peak of high nucleosome occupancy just at the center of the upstream nucleosome. This prediction agrees well with our data that showed a higher intrinsic stability of the upstream nucleosome than for the downstream nucleosome.

Different intrinsic stabilities of the two positioned nucleosomes at the *PHO84* promoter determine their differential cofactor requirement for remodeling. The *PHO84* promoter appears like a hybrid between the *PHO5* and *PHO8* promoters with regard to the cofactor dependency for chromatin remodeling upon induction. On one hand, it has a similar degree of cofactor dependency as the *PHO5* promoter, because the remodeling of the downstream nucleosome and the overall promoter activation were not essentially dependent on Snf2, Ino80, Gcn5, and Rtt109. It was not even abolished in the *snf2 ino80* or *snf2 gcn5* double mutants. Nonetheless, all these factors have a more or less important role in remodeling kinetics of the downstream nucleosome. Steger *et al.* (72) also reported a defect in *PHO84* mRNA induction in *snf6* (subunit of the SWI/SNF complex) and *arp8* (subunit of the Ino80 complex) strains, which corresponds nicely to the promoter-opening delays reported here for the *snf2* and *ino80* mutants. On the other hand, remodeling of the upstream nucleosome was reminiscent of the *PHO8* promoter, as it was strictly dependent on Snf2. In addition, it became critically dependent on Ino80 under submaximal induction conditions, while the downstream nucleosome was still remodeled, i.e., remodeling of the upstream nucleosome appeared to be more dependent on Ino80 than remodeling of the downstream nucleosome.

Therefore, the *PHO84* promoter presents an example of a differential cofactor requirement for histone eviction from two neighboring nucleosomes at the same promoter. This differen-

obtained by ExoIII mapping in the Hörz laboratory), and Barbaric *et al.* (5) (ii) with positions as determined in genome-wide studies reported by Lee *et al.* (45), Whitehouse *et al.* (82), Mavrich *et al.* (49) (fit threshold of 2 was used), Albert *et al.* (2) (those authors mapped only H2A.Z-containing nucleosomes; fit threshold of 2), and Shivaswamy *et al.* (67), and (iii) as predicted by bioinformatic algorithms of Segal *et al.* (65) and Ioshikhes *et al.* (32). The shown *N*-score algorithm of Yuan and Liu (84) is predictive for local nucleosome enrichment or depletion (positive or negative values) (Fig. 7C). Gray rectangles denote fuzzy mapping of nucleosome positioning. The midpoints of positioned nucleosomes as mapped by our own group are marked by vertical lines for orientation and their positions are denoted as stippled boxes within the *N*-score plots. For regions marked with ?-, we had no information on nucleosome positions. The positions of promoter features are labeled as in Fig. 1B and the graded horizontal line shows base pair positions relative to the ATG start codon (+1). Positions of the TSS were taken from reference 50, and positions of TATA boxes were taken from reference 9. The sHS and cHS regions of the *PHO84* promoter and hypersensitive region 2 (HS2) at the *PHO5* promoter (3) are labeled.

tial cofactor requirement poses even more poignantly the question that was raised earlier after the observation of the differential cofactor requirements at the *PHO5* and *PHO8* promoters: what makes remodeling of one nucleosome strictly dependent on a certain cofactor, for example, Snf2, while remodeling of another nucleosome is not dependent on this cofactor? In order to answer this question, the two neighboring nucleosomes at the *PHO84* promoter constitute a system that is very well internally controlled for the influence of any external factors, like cofactor recruitment, higher-order structure, or nuclear location.

One possible answer to the above question could relate to the presence of a functionally important intranucleosomal activator binding site in nucleosomes that show less cofactor dependency, like the UASpE site in the downstream nucleosome at the *PHO84* promoter or the UASp2 site in the -2 nucleosome at the *PHO5* promoter (26). However, we tested the UASpEmut, UASpCEmut, and UASpDEmut *PHO84* promoter variants in the *snf2* background under inducing conditions and saw the same sHS** $-$ -type region as for the wt *PHO84* promoter in *snf2* cells (unpublished results). Therefore, the presence of the intranucleosomal UASpE element did not influence the differential cofactor dependency for remodeling of the upstream and downstream nucleosome.

As an alternative explanation, Dhasarathy and Klade (19) showed that the stringency of cofactor requirements for chromatin remodeling at the *PHO5* promoter was dependent on the amount of Pho4 recruited to the promoter. We found this relationship also at the *PHO84* promoter, as the upstream nucleosome became critically dependent on Ino80 if less Pho4 was recruited, i.e., under submaximal inducing conditions. However, this effect is unlikely to explain the promoter-internal difference in cofactor requirements at the *PHO84* promoter under the same induction conditions. Here both the upstream and downstream nucleosome should be exposed simultaneously to the same degree of Pho4 recruitment, unless, for example, the higher-order structure makes a difference for the two nucleosomes. But this seems unlikely, as the differential Snf2 dependencies of both nucleosomes were equally observed at the plasmid and the chromosomal locus (Fig. 4B and our unpublished data), which probably differ in higher-order structures.

In this study we provide strong evidence for a hypothesis that we raised previously (31) as an answer to the above question: different intrinsic stabilities of positioned nucleosomes cause different cofactor requirements for their remodeling. We showed previously, using our yeast extract in vitro chromatin assembly system, that the nucleosomes at the *PHO8* promoter were intrinsically more stable than those at the *PHO5* promoter, thus providing a correlation of nucleosome stability and dependency on cofactors. By the same methodology we measured now a similar, although more subtle, trend while comparing the stabilities of the upstream and downstream nucleosome at the *PHO84* promoter. The former was more stably positioned than the latter. This correlated well with the prediction by the *N*-score algorithm for the *PHO84* promoter. Analogously, most of the *PHO8* promoter region had a positive prediction for nucleosome occupancy and most of the *PHO5* promoter region showed either mildly or strongly negative nucleosome propensity and the only positive peak was located

in a linker region in vivo (Fig. 10B and C). This is in agreement with our earlier notion that the nucleosomes at the repressed *PHO5* promoter adopt positions in a "loaded spring-like state" (31, 39). Altogether, it appears that nucleosomes that are positioned over DNA regions with more positive *N*-scores are more strictly dependent on chromatin cofactors for remodeling, and nucleosomes over less favorable DNA sequences according to the *N*-score can be remodeled by multiple redundant pathways.

We tested this directly for the case of the *PHO84* promoter by introducing stretches of homopolymeric poly(dA) at the position of the upstream nucleosome. This progressively lowered the *N*-score for this region. Indeed, we confirmed in the in vitro assay that the upstream nucleosome was destabilized and observed in vivo that a progressively lower stability of the upstream nucleosome allowed progressively more remodeling of this nucleosome in the absence of Snf2. Importantly, our in vitro assay was an independent measure of nucleosome stability; therefore, we needed not to invoke Snf2 dependency itself as an indicator of stability. A similar approach was undertaken at the *RNR3* promoter, where insertion of one or even two 34A stretches close to the TATA box prevented the formation of a positioned nucleosome and relieved the Snf2 dependency of *RNR3* induction (86).

We conclude that promoter strength is not necessarily correlated with the degree of cofactor requirement for chromatin remodeling but rather that intrinsic properties of individual promoter nucleosomes determine the cofactor dependency for their remodeling.

Histone eviction at the *PHO84* promoter seems to be the rate-limiting step in the absence of Gcn5 or Snf2. We and others showed previously for the *PHO5* and *PHO8* promoters that chromatin remodeling led to the eviction of histones from the promoter region (1, 14, 38). Genome-wide studies confirmed that histone-depleted regions are a common property of promoters of active genes (13, 43). As discussed earlier (14, 24, 58, 59), there is a significant mechanistic difference if remodeling of nucleosomes leads to increased DNA accessibility while histones are still present or as histones are evicted. Importantly, this distinction cannot be made by techniques based on nuclease digestion, as DNA accessibility and therefore nuclease digestibility changes in both cases. Therefore, it is not necessarily to be expected that chromatin remodeling kinetics as followed by nucleases, e.g., restriction enzyme accessibility, and by histone ChIP will coincide. Even though such kinetic measurements were congruent so far for remodeling at the *PHO5* and *PHO8* promoters (6, 8), we now observed slower kinetics of histone eviction compared to restriction enzyme accessibility kinetics during induction of the *PHO84* promoter in the *gcn5* mutant and also specifically for remodeling of the downstream nucleosome in the *snf2* mutant. This may argue for an initial phase of nucleosome remodeling leading to altered nucleosomal states that allow more restriction enzyme accessibility but still retain histones associated with DNA. This initial phase may precede the actual, rate-limiting histone eviction phase. For the *gcn5* mutation this interpretation is concordant with reports on the stimulatory effect of histone acetylation on histone eviction (17).

Rtt109 increases the rate of *PHO5* and more weakly also of *PHO84* promoter activation. The mechanism of histone evic-

tion raises the question of the histone acceptor. We and others suggested in the past that histone chaperones may be the most promising candidates as histone acceptors and showed a role for Asf1 in increasing the rate of opening of the *PHO5* and *PHO8* promoters (1, 38). However, the recognition of Asf1 as an essential cofactor for the activity of the histone H3 lysine 56-specific histone acetyltransferase Rtt109 (18, 21, 22, 30, 64, 78) raised the alternative possibility that Asf1 functions through the H3 K56ac modification rather than solely as histone acceptor. Indeed, the *PHO5* induction kinetics was equally delayed in *asf1* and *rtt109* strains, and the *asf1 rtt109* double mutant showed no synthetic effect. Very recently, just before submitting the manuscript, equivalent results were published by Williams et al. (83). So, Asf1 appears to function in histone eviction at the *PHO5* promoter mainly through H3 K56ac, and it is currently unclear if it also serves directly as a histone acceptor.

Surprisingly, in the BY4741 strain background Asf1 seemed to be hardly involved at all in *PHO84* induction despite the considerable role for Rtt109. This suggested that Rtt109 may have other targets than H3 K56. This is not unlikely, as Rtt109 exists in a complex with another histone chaperone, Vps75, that seems to be less important for acetylation of H3 K56 in vivo (12, 30, 78). The absence of Vps75 caused only a slight effect on *PHO5* induction, much weaker than that observed in the absence of Asf1, and had no significant effect on *PHO84* induction (unpublished data). Therefore, Rtt109 could function in *PHO84* induction through a so-far-unidentified target that may be acetylated by Rtt109 independently of both Asf1 and Vps75.

Chromatin cofactors have a direct effect on *PHO84* promoter regulation. All mutants used in this study (besides *rtt109*) were controlled for causing direct effects on the coregulated *PHO5* and *PHO8* promoters rather than causing side effects on PHO regulon induction (6, 8, 38). In addition, we observed decreased chromatin remodeling in the *snf2K798A* and the *ino80* mutants under steady-state conditions (overexpression of *PHO4* in +P_i medium), under which effects on growth rate should not matter, which otherwise is a concern for effects on PHO induction (6, 38). Other groups have shown a direct role for Snf2, Ino80, and Gcn5 at the *PHO84* promoter in ChIP assays (23, 36, 68, 69, 72).

Remodeling of the downstream nucleosome seems to be more important for *PHO84* promoter regulation through chromatin than remodeling of the upstream nucleosome. Even though the stable upstream nucleosome poses a very interesting case for the mechanistic study of nucleosome remodeling, it seems to have a rather minor role in the overall regulation of the *PHO84* promoter. Given its higher stability and occlusion of the UASpB site, it might play a repressive or fine-tuning role for *PHO84* regulation. However, its absence in the pCB84b construct only had a very slight effect on the promoter induction kinetics and on their Snf2 dependence. Further, full final promoter activity was achieved in the *snf2* mutant without remodeling of the upstream nucleosome. Finally, the destabilization of the upstream nucleosome in the 19A variant did relieve the Snf2 dependency for remodeling of the upstream nucleosome but had no effect on the basal level of transcription and only mild effects on the promoter induction kinetics. On the other hand, full *PHO84* promoter activity was always con-

comitant with complete remodeling of the downstream nucleosome and every delay in induction kinetics went together with a delay in its remodeling. As its intranucleosomal UASpE site was especially important for *PHO84* induction, it seems that controlling the accessibility to UASpE through remodeling of the downstream nucleosome is key to regulating *PHO84* promoter induction.

ACKNOWLEDGMENTS

We are grateful to P. D. Kaufman, C. L. Peterson, X. Shen, A. Verreault, and F. Winston for the gifts of yeast strains and to A. Schmid and to V. Fajdetic for technical assistance.

This work was supported by the German Research Community (Transregio 05), the 6th Framework Programme of the European Union (Network of Excellence The Epigenome), and the Ministry of Education, Science, and Technology of the Republic of Croatia, grant 058-0580477-0247 (to S.B.).

This paper is dedicated by P.K. to his wife Marion Rouette, who became indirectly involved enough during the preparation of the manuscript to earn her an honorary coauthorship.

REFERENCES

- Adkins, M. W., S. R. Howar, and J. K. Tyler. 2004. Chromatin disassembly mediated by the histone chaperone Asf1 is essential for transcriptional activation of the yeast *PHO5* and *PHO8* genes. *Mol. Cell* **14**:657–666.
- Albert, I., T. N. Mavrich, L. P. Tomsho, J. Qi, S. J. Zanton, S. C. Schuster, and B. F. Pugh. 2007. Translational and rotational settings of H2A.Z nucleosomes across the *Saccharomyces cerevisiae* genome. *Nature* **446**:572–576.
- Almer, A., H. Rudolph, A. Hinnen, and W. Hörz. 1986. Removal of positioned nucleosomes from the yeast *PHO5* promoter upon *PHO5* induction releases additional upstream activating DNA elements. *EMBO J.* **5**:2689–2696.
- Anderson, J. D., and J. Widom. 2001. Poly(dA-dT) promoter elements increase the equilibrium accessibility of nucleosomal DNA target sites. *Mol. Cell. Biol.* **21**:3830–3839.
- Barbaric, S., K. D. Fascher, and W. Hörz. 1992. Activation of the weakly regulated *PHO8* promoter in *S. cerevisiae*: chromatin transition and binding sites for the positive regulator protein Pho4. *Nucleic Acids Res.* **20**:1031–1038.
- Barbaric, S., T. Luckenbach, A. Schmid, D. Blaschke, W. Hörz, and P. Korber. 2007. Redundancy of chromatin remodeling pathways for the induction of the yeast *PHO5* promoter in vivo. *J. Biol. Chem.* **282**:27610–27621.
- Barbaric, S., M. Münsterkötter, C. Goding, and W. Hörz. 1998. Cooperative Pho2-Pho4 interactions at the *PHO5* promoter are critical for binding of Pho4 to UASp1 and for efficient transactivation by Pho4 at UASp2. *Mol. Cell. Biol.* **18**:2629–2639.
- Barbaric, S., J. Walker, A. Schmid, J. Q. Svejstrup, and W. Hörz. 2001. Increasing the rate of chromatin remodeling and gene activation - a novel role for the histone acetyltransferase Gcn5. *EMBO J.* **20**:4944–4951.
- Basehoar, A. D., S. J. Zanton, and B. F. Pugh. 2004. Identification and distinct regulation of yeast TATA box-containing genes. *Cell* **116**:699–709.
- Becker, P. B., and W. Hörz. 2002. ATP-dependent nucleosome remodeling. *Annu. Rev. Biochem.* **71**:247–273.
- Berger, S. L. 2007. The complex language of chromatin regulation during transcription. *Nature* **447**:407–412.
- Berndsen, C. E., T. Tsubota, S. E. Lindner, S. Lee, J. M. Holton, P. D. Kaufman, J. L. Keck, and J. M. Denu. 2008. Molecular functions of the histone acetyltransferase chaperone complex Rtt109-Vps75. *Nat. Struct. Mol. Biol.* **15**:948–956.
- Bernstein, B. E., C. L. Liu, E. L. Humphrey, E. O. Perlstein, and S. L. Schreiber. 2004. Global nucleosome occupancy in yeast. *Genome Biol.* **5**:R62.
- Boeger, H., J. Griesenbeck, J. S. Strattan, and R. D. Kornberg. 2003. Nucleosomes unfold completely at a transcriptionally active promoter. *Mol. Cell* **11**:1587–1598.
- Bun Ya, M., M. Nishimura, S. Harashima, and Y. Oshima. 1991. The *PHO84* gene of *Saccharomyces cerevisiae* encodes an inorganic phosphate transporter. *Mol. Cell. Biol.* **11**:3229–3238.
- Carvin, C. D., and M. P. Kladde. 2004. Effectors of lysine 4 methylation of histone H3 in *Saccharomyces cerevisiae* are negative regulators of *PHO5* and *GAL1-10*. *J. Biol. Chem.* **279**:33057–33062.
- Chandy, M., J. L. Gutierrez, P. Prochasson, and J. L. Workman. 2006. SWI/SNF displaces SAGA-acetylated nucleosomes. *Eukaryot. Cell* **5**:1738–1747.

18. Collins, S. R., K. M. Miller, N. L. Maas, A. Roguev, J. Fillingham, C. S. Chu, M. Schuldiner, M. Gebbia, J. Recht, M. Shales, H. Ding, H. Xu, J. Han, K. Ingvarsdottir, B. Cheng, B. Andrews, C. Boone, S. L. Berger, P. Hieter, Z. Zhang, G. W. Brown, C. J. Ingles, A. Emili, C. D. Allis, D. P. Toczyski, J. S. Weissman, J. F. Greenblatt, and N. J. Krogan. 2007. Functional dissection of protein complexes involved in yeast chromosome biology using a genetic interaction map. *Nature* **446**:806–810.
19. Dhasarathy, A., and M. P. Kladde. 2005. Promoter occupancy is a major determinant of chromatin remodeling enzyme requirements. *Mol. Cell. Biol.* **25**:2698–2707.
20. Dion, M. F., T. Kaplan, M. Kim, S. Buratowski, N. Friedman, and O. J. Rando. 2007. Dynamics of replication-independent histone turnover in budding yeast. *Science* **315**:1405–1408.
21. Driscoll, R., A. Hudson, and S. P. Jackson. 2007. Yeast Rtt109 promotes genome stability by acetylating histone H3 on lysine 56. *Science* **315**:649–652.
22. Drogaris, P., H. Wurtele, H. Masumoto, A. Verreault, and P. Thibault. 2008. Comprehensive profiling of histone modifications using a label-free approach and its applications in determining structure-function relationships. *Anal. Chem.* **80**:6698–6707.
23. Duina, A. A., and F. Winston. 2004. Analysis of a mutant histone H3 that perturbs the association of Swi/Snf with chromatin. *Mol. Cell. Biol.* **24**:561–572.
24. Eberharter, A., and P. B. Becker. 2004. ATP-dependent nucleosome remodelling: factors and functions. *J. Cell Sci.* **117**:3707–3711.
25. Fascher, K. D., J. Schmitz, and W. Hörz. 1990. Role of trans-activating proteins in the generation of active chromatin at the *PHO5* promoter in *S. cerevisiae*. *EMBO J.* **9**:2523–2528.
26. Fascher, K. D., J. Schmitz, and W. Hörz. 1993. Structural and functional requirements for the chromatin transition at the *PHO5* promoter in *Saccharomyces cerevisiae* upon *PHO5* activation. *J. Mol. Biol.* **231**:658–667.
27. Gregory, P. D., S. Barbaric, and W. Hörz. 1999. Restriction nucleases as probes for chromatin structure. *Methods Mol. Biol.* **119**:417–425.
28. Gregory, P. D., A. Schmid, M. Zavari, M. Münsterkötter, and W. Hörz. 1999. Chromatin remodelling at the *PHO8* promoter requires SWI-SNF and SAGA at a step subsequent to activator binding. *EMBO J.* **18**:6407–6414.
29. Hagenauer-Tsapis, R., and A. Hinnen. 1984. A deletion that includes the signal peptidase cleavage site impairs processing, glycosylation, and secretion of cell surface yeast acid phosphatase. *Mol. Cell. Biol.* **4**:2668–2675.
30. Han, J., H. Zhou, B. Horadzovsky, K. Zhang, R. M. Xu, and Z. Zhang. 2007. Rtt109 acetylates histone H3 lysine 56 and functions in DNA replication. *Science* **315**:653–655.
31. Hertel, C. B., G. Längst, W. Hörz, and P. Korber. 2005. Nucleosome stability at the yeast *PHO5* and *PHO8* promoters correlates with differential cofactor requirements for chromatin opening. *Mol. Cell. Biol.* **25**:10755–10767.
32. Ioshikhes, I. P., I. Albert, S. J. Zanton, and B. F. Pugh. 2006. Nucleosome positions predicted through comparative genomics. *Nat. Genet.* **38**:1210–1215.
33. Iyer, V., and K. Struhl. 1995. Poly(dA:dT), a ubiquitous promoter element that stimulates transcription via its intrinsic DNA structure. *EMBO J.* **14**:2570–2579.
34. Jamai, A., R. M. Imoberdorf, and M. Strubin. 2007. Continuous histone H2B and transcription-dependent histone H3 exchange in yeast cells outside of replication. *Mol. Cell* **25**:345–355.
35. Jeffery, D. A., M. Springer, D. S. King, and E. K. O'Shea. 2001. Multi-site phosphorylation of Pho4 by the cyclin-CDK Pho80-Pho85 is semi-processive with site preference. *J. Mol. Biol.* **306**:997–1010.
36. Jonsson, Z. O., S. Jha, J. A. Wohlschlegel, and A. Dutta. 2004. Rvb1p/Rvb2p recruit Arp5p and assemble a functional Ino80 chromatin remodeling complex. *Mol. Cell* **16**:465–477.
37. Kaffman, A., I. Herskowitz, R. Tjian, and E. K. O'Shea. 1994. Phosphorylation of the transcription factor Pho4 by a cyclin-CDK complex, Pho80-Pho85. *Science* **263**:1153–1156.
38. Korber, P., S. Barbaric, T. Luckenbach, A. Schmid, U. J. Schermer, D. Blaschke, and W. Hörz. 2006. The histone chaperone Asf1 increases the rate of histone eviction at the yeast *PHO5* and *PHO8* promoters. *J. Biol. Chem.* **281**:5539–5545.
39. Korber, P., and W. Hörz. 2004. In vitro assembly of the characteristic chromatin organization at the yeast *PHO5* promoter by a replication-independent extract system. *J. Biol. Chem.* **279**:35113–35120.
40. Kouzarides, T. 2007. Chromatin modifications and their function. *Cell* **128**:693–705.
41. Lam, F. H., D. J. Steger, and E. K. O'Shea. 2008. Chromatin decouples promoter threshold from dynamic range. *Nature* **453**:246–250.
42. Längst, G., E. J. Bonte, D. F. Corona, and P. B. Becker. 1999. Nucleosome movement by CHRAC and ISWI without disruption or trans-displacement of the histone octamer. *Cell* **97**:843–852.
43. Lee, C. K., Y. Shibata, B. Rao, B. D. Strahl, and J. D. Lieb. 2004. Evidence for nucleosome depletion at active regulatory regions genome-wide. *Nat. Genet.* **36**:900–905.
44. Lee, T. I., H. C. Causton, F. C. Holstege, W. C. Shen, N. Hannett, E. G. Jennings, F. Winston, M. R. Green, and R. A. Young. 2000. Redundant roles for the TFIID and SAGA complexes in global transcription. *Nature* **405**:701–704.
45. Lee, W., D. Tillo, N. Bray, R. H. Morse, R. W. Davis, T. R. Hughes, and C. Nislow. 2007. A high-resolution atlas of nucleosome occupancy in yeast. *Nat. Genet.* **39**:1235–1244.
46. Li, B., M. Carey, and J. L. Workman. 2007. The role of chromatin during transcription. *Cell* **128**:707–719.
47. Liu, X., C. K. Lee, J. A. Granek, N. D. Clarke, and J. D. Lieb. 2006. Whole-genome comparison of Leu3 binding in vitro and in vivo reveals the importance of nucleosome occupancy in target site selection. *Genome Res.* **16**:1517–1528.
48. Luger, K., A. W. Mader, R. K. Richmond, D. F. Sargent, and T. J. Richmond. 1997. Crystal structure of the nucleosome core particle at 2.8 Å resolution. *Nature* **389**:251–260.
49. Mavrich, T. N., I. P. Ioshikhes, B. J. Venters, C. Jiang, L. P. Tomsho, J. Qi, S. C. Schuster, I. Albert, and B. F. Pugh. 2008. A barrier nucleosome model for statistical positioning of nucleosomes throughout the yeast genome. *Genome Res.* **18**:1073–1083.
50. Miura, F., N. Kawaguchi, J. Sese, A. Toyoda, M. Hattori, S. Morishita, and T. Ito. 2006. A large-scale full-length cDNA analysis to explore the budding yeast transcriptome. *Proc. Natl. Acad. Sci. USA* **103**:17846–17851.
51. Morse, R. H. 2007. Transcription factor access to promoter elements. *J. Cell. Biochem.* **102**:560–570.
52. Münsterkötter, M., S. Barbaric, and W. Hörz. 2000. Transcriptional regulation of the yeast *PHO8* promoter in comparison to the coregulated *PHO5* promoter. *J. Biol. Chem.* **275**:22678–22685.
53. Neef, D. W., and M. P. Kladde. 2003. Polyphosphate loss promotes SNF/SWI- and Gcn5-dependent mitotic induction of *PHO5*. *Mol. Cell. Biol.* **23**:3788–3797.
54. Ogawa, N., H. Saitoh, K. Miura, J. P. V. Magbanua, M. Bunya, S. Harashima, and Y. Oshima. 1995. Structure and distribution of specific cis-elements for transcriptional regulation of *PHO84* in *Saccharomyces cerevisiae*. *Mol. Gen. Genet.* **249**:406–416.
55. Oshima, Y. 1997. The phosphatase system in *Saccharomyces cerevisiae*. *Genes Genet. Syst.* **72**:323–334.
56. Park, Y. J., and K. Luger. 2008. Histone chaperones in nucleosome eviction and histone exchange. *Curr. Opin. Struct. Biol.* **18**:282–289.
57. Prunell, A. 1982. Nucleosome reconstitution on plasmid-inserted poly(dA)_npoly(dT). *EMBO J.* **1**:173–179.
58. Reinke, H., and W. Hörz. 2003. Histones are first hyperacetylated and then lose contact with the activated *PHO5* promoter. *Mol. Cell* **11**:1599–1607.
59. Reinke, H., and W. Hörz. 2004. Anatomy of a hypersensitive site. *Biochim. Biophys. Acta* **1677**:24–29.
60. Richmond, E., and C. L. Peterson. 1996. Functional analysis of the DNA-stimulated ATPase domain of yeast SWI2/SNF2. *Nucleic Acids Res.* **24**:3685–3692.
61. Roberts, S. M., and F. Winston. 1997. Essential functional interactions of SAGA, a *Saccharomyces cerevisiae* complex of Spt, Ada, and Gcn5 proteins, with the Snf-Swi and Srb-mediator complexes. *Genetics* **147**:451–465.
62. Rufiang, A., P. E. Jacques, W. Bhat, F. Robert, and A. Nourani. 2007. Genome-wide replication-independent histone H3 exchange occurs predominantly at promoters and implicates H3 K56 acetylation and Asf1. *Mol. Cell* **27**:393–405.
63. Sarkar, G., and S. S. Sommer. 1990. The “megaprimer” method of site-directed mutagenesis. *BioTechniques* **8**:404–407.
64. Schneider, J., P. Bajwa, F. C. Johnson, S. R. Bhaumik, and A. Shilatifard. 2006. Rtt109 is required for proper H3K56 acetylation: a chromatin mark associated with the elongating RNA polymerase II. *J. Biol. Chem.* **281**:37270–37274.
65. Segal, E., Y. Fondufe-Mittendorf, L. Chen, A. Thastrom, Y. Field, I. K. Moore, J. P. Wang, and J. Widom. 2006. A genomic code for nucleosome positioning. *Nature* **442**:772–778.
66. Shen, X., G. Mizuguchi, A. Hamiche, and C. Wu. 2000. A chromatin remodeling complex involved in transcription and DNA processing. *Nature* **406**:541–544.
67. Shivaswamy, S., A. Bhingre, Y. Zhao, S. Jones, M. Hirst, and V. R. Iyer. 2008. Dynamic remodeling of individual nucleosomes across a eukaryotic genome in response to transcriptional perturbation. *PLoS Biol.* **6**:e65.
68. Shukla, A., P. Bajwa, and S. R. Bhaumik. 2006. SAGA-associated Sgf73p facilitates formation of the preinitiation complex assembly at the promoters either in a HAT-dependent or independent manner in vivo. *Nucleic Acids Res.* **34**:6225–6232.
69. Shukla, A., N. Stanojevic, Z. Duan, P. Sen, and S. R. Bhaumik. 2006. Ubp8p, a histone deubiquitinase whose association with SAGA is mediated by Sgf11p, differentially regulates lysine 4 methylation of histone H3 in vivo. *Mol. Cell. Biol.* **26**:3339–3352.
70. Simon, R. H., and G. Felsenfeld. 1979. A new procedure for purifying histone pairs H2A + H2B and H3 + H4 from chromatin using hydroxylapatite. *Nucleic Acids Res.* **6**:689–696.
71. Springer, M., D. D. Wykoff, N. Miller, and E. K. O'Shea. 2003. Partially phosphorylated Pho4 activates transcription of a subset of phosphate-responsive genes. *PLoS Biol.* **1**:e28.

72. Steger, D. J., E. S. Haswell, A. L. Miller, S. R. Wente, and E. K. O'Shea. 2003. Regulation of chromatin remodeling by inositol polyphosphates. *Science* **299**:114–116.
73. Strahl-Bolsinger, S., A. Hecht, K. Luo, and M. Grunstein. 1997. SIR2 and SIR4 interactions differ in core and extended telomeric heterochromatin in yeast. *Genes Dev.* **11**:83–93.
74. Svaren, J., and W. Hörz. 1997. Transcription factors vs nucleosomes: regulation of the *PHO5* promoter in yeast. *Trends Biochem. Sci.* **22**:93–97.
75. Svaren, J., J. Schmitz, and W. Hörz. 1994. The transactivation domain of Pho4 is required for nucleosome disruption at the *PHO5* promoter. *EMBO J.* **13**:4856–4862.
76. Svaren, J., U. Venter, and W. Hörz. 1995. *In vivo* analysis of nucleosome structure and transcription factor binding in *Saccharomyces cerevisiae*. *Microb. Gene Tech.* **6**:153–167.
77. Thomas, M. R., and E. K. O'Shea. 2005. An intracellular phosphate buffer filters transient fluctuations in extracellular phosphate levels. *Proc. Natl. Acad. Sci. USA* **102**:9565–9570.
78. Tsubota, T., C. E. Berndsen, J. A. Erkmann, C. L. Smith, L. Yang, M. A. Freitas, J. M. Denu, and P. D. Kaufman. 2007. Histone H3-K56 acetylation is catalyzed by histone chaperone-dependent complexes. *Mol. Cell* **25**:703–712.
79. Tsukiyama, T. 2002. The *in vivo* functions of ATP-dependent chromatin-remodelling factors. *Nat. Rev. Mol. Cell Biol.* **3**:422–429.
80. Venter, U., J. Svaren, J. Schmitz, A. Schmid, and W. Hörz. 1994. A nucleosome precludes binding of the transcription factor Pho4 *in vivo* to a critical target site in the *PHO5* promoter. *EMBO J.* **13**:4848–4855.
81. Wechsler, M. A., M. P. Kladde, J. A. Alfieri, and C. L. Peterson. 1997. Effects of Sin- versions of histone H4 on yeast chromatin structure and function. *EMBO J.* **16**:2086–2095.
82. Whitehouse, L., O. J. Rando, J. Delrow, and T. Tsukiyama. 2007. Chromatin remodelling at promoters suppresses antisense transcription. *Nature* **450**:1031–1035.
83. Williams, S. K., D. Truong, and J. K. Tyler. 2008. Acetylation in the globular core of histone H3 on lysine-56 promotes chromatin disassembly during transcriptional activation. *Proc. Natl. Acad. Sci. USA* **105**:9000–9005.
84. Yuan, G. C., and J. S. Liu. 2008. Genomic sequence is highly predictive of local nucleosome depletion. *PLoS Comput. Biol.* **4**:e13.
85. Yuan, G. C., Y. J. Liu, M. F. Dion, M. D. Slack, L. F. Wu, S. J. Altschuler, and O. J. Rando. 2005. Genome-scale identification of nucleosome positions in *S. cerevisiae*. *Science* **309**:626–630.
86. Zhang, H., and J. C. Reese. 2007. Exposing the core promoter is sufficient to activate transcription and alter coactivator requirement at RNR3. *Proc. Natl. Acad. Sci. USA* **104**:8833–8838.